Water Air Soil Pollut (2026) 237:436
https://doi.org/10.1007/s11270-026-09094-z

Spatiotemporal Heterogeneity and Spatial Aggregation Characteristics of $PM_{2.5}$ and O_3 in Southwest China: Evidence from a Mega Mountain City

Xiaoju Li · Luqman Chuah Abdullah · Jinzhao Hu · Shafreeza Sobri · Mohamad Syazarudin Md Said · Siti Aslina Hussain · Tan Poh Aun

Received: 17 October 2024 / Accepted: 5 January 2026 / Published online: 22 January 2026

Abstract Cities are the basic administrative units for formulating and implementing policies to reduce pollution and carbon dioxide. This study used statistical analysis and Kriging interpolation to clarify the spatiotemporal fluctuation characteristics of $PM_{2.5}$ and O_3 at different time scales in Chongqing from 2017 to 2022. It also explored the compliance rate of pollutants and their correlation. In addition, GeoDa software was used to examine the spatial autocorrelation and clustering of pollutants. Finally, relevant measures and suggestions were put forward from different perspectives of provinces, cities, districts and counties. The results showed that $PM_{2.5}$ and O_3 pollutions were still particularly serious and there was a complex linear interaction between them. Furthermore, $PM_{2.5}$ and O_3 both have significant positive spatial autocorrelation and aggregation characteristics, and their high-high agglomeration areas are mainly concentrated in the city proper of Chongqing. These results can provide potential guidance for developing differentiated and refined air pollution prevention and control measures in the region, thereby promoting the continuous improvement of regional air quality. More importantly, it can provide a reference for the practice of collaborative carbon pollution reduction and regional collaborative emission reduction in China's megacities. It also provide insights and methods that can be applied to other countries (WHO: World Health Organization; SCB: Sichuan Basin; NAAQS: National Ambient Air Quality Standards of China;

Supplementary Information The online version contains supplementary material available at https://doi.org/10.1007/s11270-026-09094-z.

X. Li
Xichang University, No. 1 Xuefu Road, Anning Town, Xichang City 615013, Sichuan Province, China

X. Li · L. C. Abdullah · S. Sobri · M. S. M. Said · S. A. Hussain
Department of Chemical and Environmental Engineering, Faculty of Engineering, University Putra Malaysia, 43400 UPM, Serdang, Selangor, Malaysia

L. C. Abdullah (✉)
Institute of Tropical Forestry and Forest Products, Universiti Putra Malaysia, UPM, 43400 Serdang, Selangor, Malaysia
e-mail: chuah@upm.edu.my

J. Hu
Neijiang Normal University, No. 1 Hongqiao Street, Dongxing District, Neijiang, City 641100, Sichuan Province, China

T. P. Aun
SOx NOx Asia Sdn Bhd, UEP, 47620 Subang Jaya, Selangor Darul Ehsan, Malaysia

MEIC: Multi-resolution Emission Inventory for China; VOCs: Volatile Organic Compounds).

Keywords Spatial-temporal heterogeneity · Spatial autocorrelation · Moran's Index · Spatial aggregation effects · Synergy effect · Differentiated and refined measures

1 Introduction

Rapid global economic growth, urban expansion, and accelerated industrialization have led to the emission of large amounts of air pollutants around the world (Martori et al.,2022; Shi et al.,2020). This has made air pollution a common urban environmental problem facing the world (Huynh et al., 2023; Rahman et al., 2021; Song et al., 2022). Air pollution has the characteristics of diversity and complexity, which lead to a series of ecological and environmental effects, endangers human health, and threatens sustainable economic and social development (Bai et al., 2022a, b; Boniardi et al., 2023). Numerous cities around the world are encountering a development bottleneck due to air pollution. About 99% of the population in 97% of the world's cities breathe air that exceeds World Health Organization (WHO) guidance limits (Kazemi Shariat Panahi et al., 2022; Liu et al., 2023). In addition, air pollution ranks as the fourth cause of death in the world and is closely related to cardiovascular disease morbidity and mortality (Luo et al., 2022; Montone et al., 2023). Global Burden of Disease of 2019 shows more than 7 million premature deaths in China, about 26% of which are attributable to $PM_{2.5}$ and O_3 exposure (Shi et al., 2021).

In the short term, China's carbon dioxide emissions are on an upward trend and still rank first in the world (Fig. 1) (Li et al., 2021b; Wang et al., 2019; Zhao et al., 2019). Currently, China faces the dual challenges of improving air quality and addressing climate change, and also pledged to achieve the peak of carbon dioxide emissions by 2030 and to realize carbon neutrality by 2060 (Energy Foundation China, 2020). China's air pollution prevention and control has reached a deep water areas and is in the stage of coordinated control of O_3, $PM_{2.5}$ and carbon emissions (Feng et al., 2023a, b); Li et al., 2023; Tang et al., 2022). Previous studies have found that driven by factors such as climate change, China's surface O_3 and $PM_{2.5}$ pollution hazards will become more serious (Huynh et al., 2023; Luo et al., 2022; Qi et al., 2023). In 2022, the average proportion of days with good air quality in China's 339 cities at prefecture level and above was 86.5%, while the average O_3 concentration was 145 μg/m^3, a year-on-year increase of 5.8% (Ji et al., 2024; Yang et al., 2023; Yi et al., 2022). Relevant projections show that the number of premature deaths caused by $PM_{2.5}$ will reached 1.59 million deaths in 2030 and about 13.44 million premature deaths in 2100 (China Clean Air Policy Partnership, 2021).

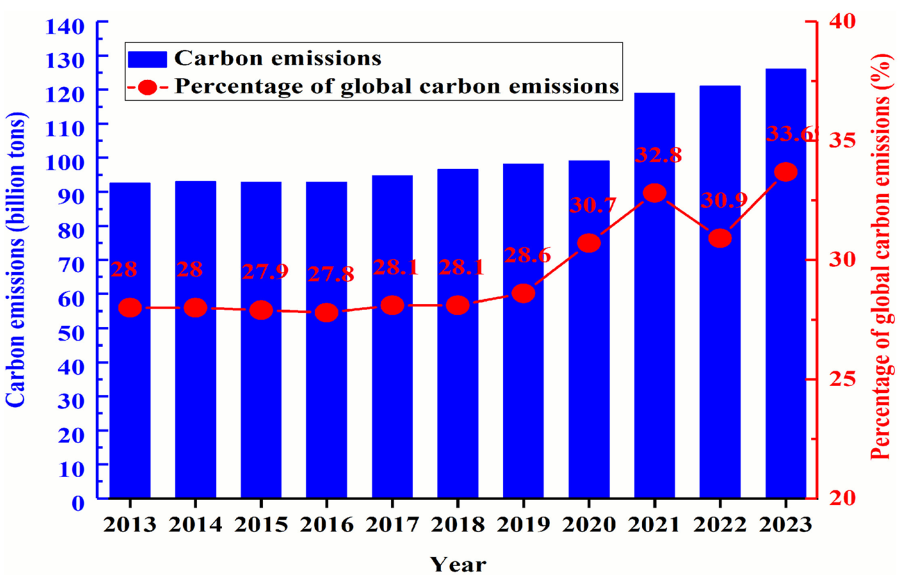

Fig. 1 China's carbon emissions 2013-2023 (Source: http://meicmodel.org.cn)

During China's "14th Five-Year Plan" period, it is necessary to highlight shortcomings and strengthen coordinated control of $PM_{2.5}$ and O_3 (Feng et al., 2019; Lin et al., 2022; Wu et al., 2021). In December 2023, the State Council of China issued the "Action Plan for Continuous Improvement of Air Quality", which focuses on improving air quality and emphasizes the coordinated control of $PM_{2.5}$ and O_3 (Feng et al., 2023a), b); Peng et al., 2020). In addition, existing studies have demonstrated that severe air pollution occurs frequently in highly industrialized and urbanized cities with complex terrains (basins and mountains), such as Beijing, Lanzhou and Chongqing in China (Dong et al., 2018; Liu et al., 2022). Numerous studies have shown that governments face greater challenges in improving air quality in the Sichuan Basin (SCB) (Ning et al., 2018; Xu et al., 2018). Therefore, it is particularly important to pay more attention to and fully understand the current pollution situation and research progress in Chengdu and Chongqing (Ding et al., 2022; Wang et al., 2020; Zhang et al., 2022). The unique basin topography and complex meteorological conditions impedes the diffusion and migration of local pollutants, making the pollution problems in these two megacities particularly severe (Fan et al., 2020; Tian et al.,2019; Xu et al., 2020; Zhang et al., 2019). From 2013 to 2017, the chronic per capita mortality rate (1.4‰) in Chongqing caused by $PM_{2.5}$ ranked first in China (Wang et al., 2020).

Many scholars have explored the current situation, causes, distribution characteristics and chemical composition of air pollution in SCB from different perspectives (Deng et al., 2022a, b); Hu et al., 2022; Qiao et al., 2021; Zhang et al., 2022). Even for the same research subjects, there may be significant bias in the results due to differences in parameters and methods discussed (Liu et al., 2021). What's more, most of the existing studies focus on specific pollution events and the research time is relatively short. Therefore, it is difficult for some existing studies to accurately characterize the long-term pollution status of these two megacities. The spatial and temporal changes of O_3 and $PM_{2.5}$ composite pollution in Chongqing and their possible internal relationships have not yet been systematically evaluated. In the long term, there are still many unknowns about the spatiotemporal heterogeneity of pollutants in Chongqing's megacities. In addition, there is relatively limited research on the long-term spatiotemporal variation characteristics of $PM_{2.5}$ and O_3 pollutants in this megacity from the perspective of districts and counties. Further exploration of the spatial autocorrelation effects of air pollutants in Chongqing is a topic that cannot be ignored in the research directions of environment, energy and economy. However, few studies have focused on the spatial distribution pattern of pollutants over long periods of time in this mountainous megacity in the SCB.

In view of the limitations of previous research, such as limited research scope, short time series, this paper analyzes the long-term (2017-2022) spatiotemporal variation patterns of $PM_{2.5}$ and O_3 in Chongqing from different perspectives. Specifically, (1) Focus on analyzing the temporal characteristics of $PM_{2.5}$ and O_3 at different time scales, and deeply explore the compliance rates of $PM_{2.5}$ and O_3 as well as the Pearson correlation between them; (2) The annual spatial distribution maps of $PM_{2.5}$ and O_3 were discussed using ArcGIS interpolation analysis; (3) Combined with GeoDa software, the spatial autocorrelation of $PM_{2.5}$ and O_3 during the long-term period was tested based on the global Moran's I statistic; (4) The spatial aggregation areas, aggregation type and detailed distribution of $PM_{2.5}$ and O_3 in various districts and counties were explored through local Moran's I analysis. The main contribution of this study is to provide a more detailed long-term analysis of the spatial effects of typical mountainous megacities. This allows for a more accurate assessment of pollutant emissions at the district and county levels. In addition, it will help the Chengdu-Chongqing region achieve its "dual carbon" goals by providing refined and targeted emission reduction policies and control suggestions. It will also provide an action guide for China to comprehensively coordinate and promote coordinated carbon pollution reduction, and further promote the comprehensive green transformation of China's economy.

2 Methodology

2.1 Study Area

Chongqing is one of the four major municipalities in China and located in southwest China (E105°11'~110°11', N28°10'~32°13') (Ding et al., 2022; Qiao et al., 2019). It covers an area of 82,400 square kilometers, which is much larger than China's megacities such as Beijing and Shanghai (Table 1). There are 38 county-level administrative regions, which can be divided into "one district and two clusters" (Fig. 2) (Feng et al., 2023a, b); Su et al., 2018). The city is mainly mountainous (76%), followed by hilly areas (22%), and only some areas are flat valleys (2%) (Ding et al., 2022). The terrain is high in the southeast and northeast, low in the middle and west, and gradually decreases from the north to the south along the Yangtze River Valley (Fig. 2). It is known as a "mountain city" and "Fog City" and is a model of mountain cities in China. In addition, the region has a subtropical monsoon climate. Its main climatic characteristics are abundant precipitation (annual average relative humidity of 70%~80%), cloudy and foggy weather, and frequent meteorological disasters (Ding et al., 2022; Ji et al., 2019; Zhang et al., 2022). Since the spatial differences in county economic development are very significant, this study selected 38 districts and counties in Chongqing as the basic research units.

2.2 Data Sources and Processing

This study mainly explores the spatiotemporal heterogeneity and aggregation characteristics of O_3

Table 1 Overview of the development of typical megacities in China (2022) (Source: http://www.stats.gov.cn/)

Megacities	Area (sq. km)	Permanent resident population (10 000 persons)	GDP per capita (100 million yuan)	Urbanization rate (%)
Beijing	16411	2184.3	41610.9	87.6
Shanghai	6341	2475.9	44652.8	89.3
Tianjing	11917	1363.0	16311.3	85.1
Shenzheng	1997	1766.2	32387.7	99.8
Chengdu	14335	2126.8	20817.5	79.9
Chongqing	82269	3213.3	29129.0	71.0

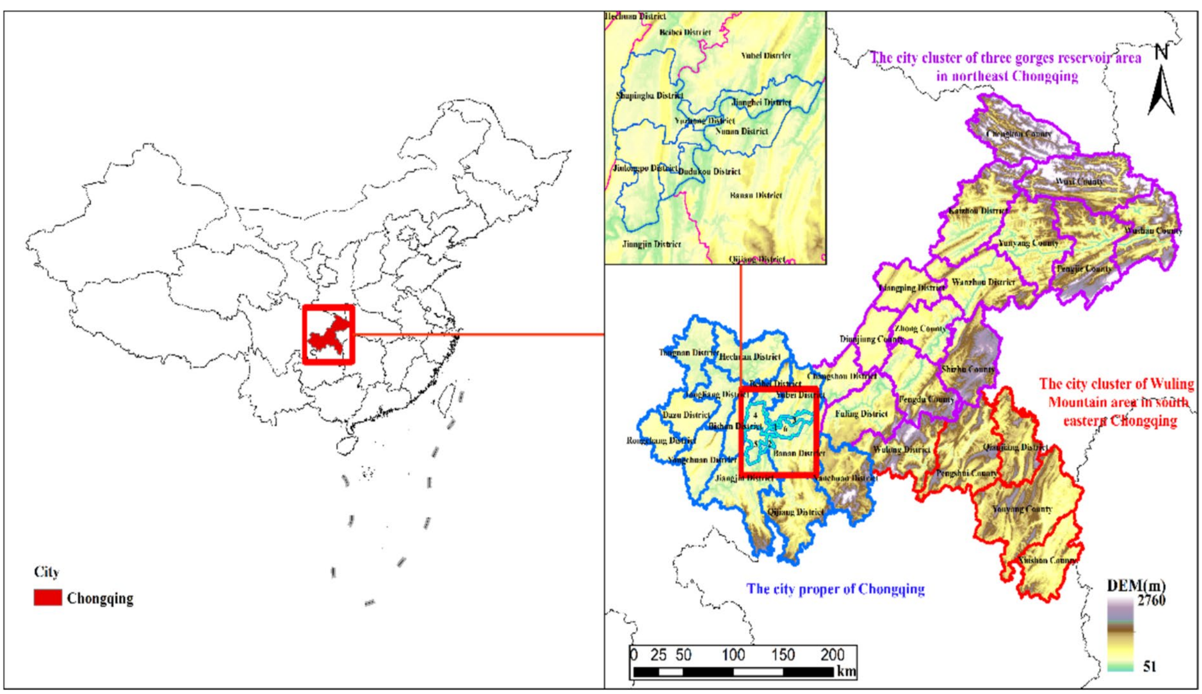

Fig. 2 Chongqing geographical location

and $PM_{2.5}$ in Chongqing and the main data involved include air pollutants data, natural factor data set, and socioeconomic data (Table S1) (Chen et al., 2022; Ma et al., 2024; Zhan et al., 2019). In addition, the "daily average", "monthly average" and "annual average" of the pollutants and other data involved are processed with reference to MEP (http://www.zhb.gov.cn/). In addition, the distribution of pollutants at different time scales in Chongqing mainly refers to the National Ambient Air Quality Standards of China (NAAQS) and the WHO introduced concentration limits (Table S2). It also referenced the Technical Regulation on Ambient Air Quality Index of China (HJ633-2012) (Table 2). The spatial analysis of pollutants in the study was mainly completed by kriging interpolation using ArcGIS (version 10.8). The spatial autocorrelation of pollutants was verified using the GeoDa platform combined with ArcGIS. At the same time, other related analysis and charting were conducted through Excel, SPSS, Minitab and Origin statistical software.

2.3 Research Methodology

2.3.1 Pearson Correlation Coefficient

Correlation analysis is an effective method to identify the strength of the relationship between two random variables, among which Pearson, Ken-dall and Spearman are the most widely used (Ai et al., 2024; Rahman et al., 2021; Xiao et al., 2023). In addition, Pearson is more suitable for continuous numerical variables. In this study, the Pearson correlation coefficient was utilized to explore the relationships between $PM_{2.5}$ and O_3 concentrations. The mathematical expression is as Eq. (1), X_i and Y_i represent the daily average $PM_{2.5}$ and O_3 concentrations on the i^{th} day, respectively. The coefficient ranges from −1 to +1. The closer the value is to ±1, the stronger the positive or negative correlation between the two variables, while R=0 indicates no linear correlation (Feng & Fang, 2022; Han et al., 2023).

$$R = \frac{\sum_{i=1}^{n}\left(X_i - \overline{X}\right)\left(Y_i - \overline{Y}\right)}{\sqrt{\sum_{i=1}^{n}\left(X_i - \overline{X}\right)^2}\sqrt{\sum_{i=1}^{n}\left(Y_i - \overline{Y}\right)^2}} \tag{1}$$

2.3.2 Kriging Interpolation

For monitoring point data with spatial autocorrelation, the complete spatial distribution in the entire area can be understood through interpolation. The spatial interpolation method is an important method for visually studying the regional distribution characteristics of air quality. Currently, the most commonly used spatial interpolation methods in the analysis of air quality distribution characteristics include inverse distance (IDW) interpolation and kriging interpolation (Fan et al., 2024; Kumar et al., 2022; Tamir & Atallel, 2023). Kriging interpolation analysis is an interpolation method based on statistics, which is suitable for the study of regionalized variables with spatial correlation (Gao et al., 2022). Compared with other interpolation methods, this interpolation method takes into account both the spatial position relationship between points and the spatial autocorrelation relationship of attribute variables between known points (Han et al., 2023; Tamir & Atallel, 2023). Therefore, the interpolation results are more consistent with the variation patterns of attribute variables in the study area. Kriging interpolation can be expressed as Eq (2), where $z^*(x_0)$ is the estimated value at the interpolation point x_0; $z(x_i)$ is the observed value at x_i among the n sample points; λ_i is the corresponding weight. The

Table 2 $PM_{2.5}$ and O_3 concentration classification

Grades	$PM_{2.5}$ pollution concentration	O_3 pollution concentration
Excellent	≤ 35 μg/m^3	≤ 100 μg/m^3
Good	35.01–75.00 μg/m^3	100.01–160.00 μg/m^3
Mild pollution	75.01–115 μg/m^3	160.01–215.00 μg/m^3
Moderate pollution	115.01–150 μg/m^3	215.01–265.00 μg/m^3
Heavy pollution	150.01–250.01 μg/m^3	265.01–800.00 μg/m^3
Severely pollution	≥250μg/m^3	≥800μg/m^3

Kriging interpolation method needs to satisfy two conditions: unbiasedness (Eq (3)) and minimum estimated variance (Eq (4)) (Han et al., 2023; Ran et al., 2020; Wong et al., 2023).

$$z^*(x_0) = \sum_{i=1}^{n} \lambda_i z(x_i) \tag{2}$$

$$E\left[z(x_0) - z^*(x_0)\right] = 0 \tag{3}$$

$$Var\left[z(x_0) - z^*(x_0)\right] = \min \tag{4}$$

Kriging interpolation is one of the most commonly used methods in the spatial characteristics analysis of air pollutants at the city scale. It includes ordinary kriging, general kriging, and simple kriging, etc. Ordinary kriging is mainly suitable for most spatial data without obvious global trends, and it is also the most commonly used and basic method. General kriging is often used when the data exhibits a clear global trend. Simple kriging typically assumes that the overall mean of the study area is a known constant, and this method is less commonly used. Based on the uncertainty of pollutant change trends, this study chose the ordinary kriging method to draw spatial distribution maps of $PM_{2.5}$ and O_3 pollutants, and then explored their spatiotemporal variation characteristics. In addition, common semivariogram models in the Kriging method include the spherical model, the exponential model, and the Gaussian model. The spherical model is the most commonly used and can well describe phenomena with a defined spatial correlation range. The exponential model usually indicates that spatial correlation gradually decreases with distance, while the Gaussian model is suitable for phenomena with very smooth spatial variations. This study compared the cross-validation results under different semivariogram models using the root mean square error (RMSE) and selected the spherical model (with the smallest RMSE) as the optimal interpolation model.

2.3.3 Spatial Autocorrelation Analysis

Global Spatial Autocorrelation As regional air pollutant emissions have the characteristics of spatial spillover and spatial diffusion, air pollution has significant spatial autocorrelation (Wang et al., 2023; Zhao et al., 2022). Spatial autocorrelation analysis is a statistical method used to reveal the aggregation characteristics of geographical entities or attributes in spatial distribution, including global and local spatial autocorrelation (Liu et al., 2022). Global spatial autocorrelation expresses the spatial aggregation or dispersion of attribute values in a specific area. This study uses the global Moran's I index to determine the aggregation or discrete characteristics of urban air pollutants in geographical space, thereby determining whether there is spatial agglomeration of urban air quality in the study area, which can be calculated by Eq. (5). The global Moran's I index can reflect the overall spatial autocorrelation of the research unit, and the value of I is [−1,1] (Xu et al., 2022). The closer Moran's I value is to 1, the stronger the positive autocorrelation of spatial distribution. This means that the distribution of O_3 and $PM_{2.5}$ in various districts and counties of Chongqing has a more obvious clustering characteristic. If it is closer to −1, it indicates that the distribution of the pollutants in the city has more prominent discrete characteristics (Wang et al., 2020; Xu et al., 2022). When I is equal to 0, it indicates that the distribution of urban $PM_{2.5}$ and O_3 shows random distribution characteristics. In addition, the P value in autocorrelation analysis can determine the reliability of the dataset, while the Z value and I value are used to distinguish the degree of clustering or dispersion patterns of the dataset (Si et al., 2024; Wang et al., 2023; Xu et al., 2022).

$$Moran's\ I = \frac{n \sum_{i=1}^{n} \sum_{j=1}^{n} W_{ij}(y_i - y)(y_j - y)}{\sum_{i=1}^{n} \sum_{j=1}^{n} W_{ij} \sum_{i=1}^{n} (y_i - y)^2} \tag{5}$$

In the formula, n represents the number of counties in the study region, y_i and y_j represent the average concentration of pollutants in study area i and study area j, y represents the average concentration of pollutants in all areas, and W_{ij} represents the spatial weight matrix between study areas i and j (Wang et al., 2020; Xu et al., 2022). Common methods for constructing spatial weight matrices include the distance threshold method, the inverse distance method, or the k-nearest neighbor method. Based on the characteristics of Chongqing's complex terrain, uneven distribution of monitoring stations, and nonlinear decay of pollutant diffusion, this study uses the inverse distance weighting method in spatial autocorrelation analysis. Meanwhile, to ensure the accuracy and comparability of the spatial autocorrelation analysis, the constructed spatial weight matrix was row-standardized. Furthermore, to more accurately reflect the physical process of pollutant concentration continuously decreasing with distance, continuous weights were used in the analysis. Finally, in order to verify the significance level of spatial autocorrelation, calculate the standardized statistic Z(I) as Eq. (6). Where E(I) and Var(I) represent the expected value and standard deviation of Moran's I, respectively (Si et al., 2024; Wang et al., 2023; Xu et al., 2022).

$$Z(I) = 1 - E(I)/\sqrt{Var(I)} \tag{6}$$

Local Spatial Autocorrelation Global spatial autocorrelation can only reflect the spatial aggregation phenomenon but cannot observe the specific location of similar clustering areas. Therefore, the local Moran's I index is used to further identify the detailed information of the spatial autocorrelation area and measured by the spatially correlated local index LISA. LISA analysis can be used as a basis to judge the diffusion, migration and spatial correlation of pollutants, and to explore the potential changing trends of air pollution and severely polluted areas (Dettori et al., 2021; Mi et al., 2024; Yang et al., 2024). This research use Moran's I as an index to clarify the local spatial correlation of $PM_{2.5}$ and O_3, which is defined as Eq. (7). Among them, n indicates the number of study areas; x_j and x_j expressed the observed values of pollutants in units i and j respectively; $\overline{x}$ is the average value of x; W_{ij} is the spatial weight matrix element (Wang et al., 2021; Zhan et al., 2019).

$$Local\ Moran's\ I = \frac{n\left(x_i - \overline{x}\right)\sum_{j=1}^{n} W_{ij}\left(x_j - \overline{x}\right)}{\sum_{i=1}^{n}\left(x_i - \overline{x}\right)^2} \tag{7}$$

The significance test uses the standardized statistic Z to test, and the Z expression is consistent with the global autocorrelation Eq. (6) (Wang et al., 2021; Zhan et al., 2019). That is, the horizontal and vertical axes of the Moran scatter plot are standardized (Z-score standardized) variable values. The horizontal axis Z (Variable) represents the standardized value of the original observations for each spatial cell. The vertical axis WZ (Variable) represents the standardized value of the weighted average of the neighborhood values for each spatial cell. Combined with the Z test, four statistically significant spatial correlation patterns can be detected as shown in Fig. 3.The autocorrelations in the first and third quadrants (HH and LL) are positive, and those in the second and fourth quadrants (LH or HL) are negative (Ma et al., 2019; Ren & Matsumoto, 2020; Wang et al., 2020). The specific meanings of the four quadrants are as follows: (1) HH (Z>0): Hotspot/clustered area, indicating that a high-value area is surrounded by other high-value areas. For example, an area with high $PM_{2.5}/O_3$ concentrations is surrounded by other areas with high $PM_{2.5}/O_3$ concentrations. (2) LL (Z<0): Cold spot area/cluster area, indicating that a low-value area is surrounded by other low-value areas. (3) LH (Z<0): Low value surrounded by high value, indicating that a low-value cell is surrounded by high-value neighbors. For example, an area with low $PM_{2.5}/O_3$ concentration is surrounded by other areas with high $PM_{2.5}/O_3$ concentration. (4) HL (Z>0): Areas where high values are surrounded by low values, indicating that a high-value cell is surrounded by its low-value neighbors.

3 Results and Discussion

3.1 Temporal Evolution Characteristics of $PM_{2.5}$ and O_3

3.1.1 Temporal Variation Characteristics in Districts and Counties

Although the $PM_{2.5}$ concentration in Chongqing has generally shown a downward trend in recent years,

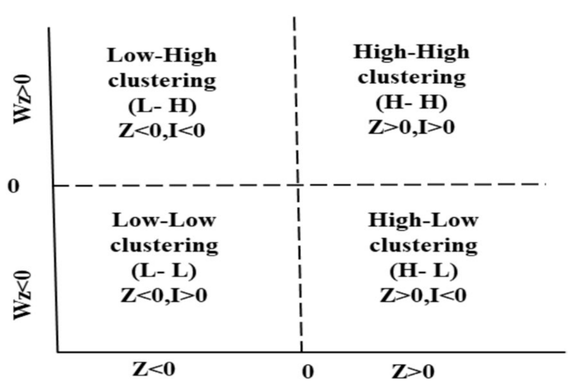

Fig. 3 The quadrant parsing of Moran scatterplot

the O_3 pollution problem has gradually become more prominent (Tan et al., 2023; Wang et al., 2020). Exploring the pollution trends of $PM_{2.5}$ and O_3 from the fperspective of districts and counties will help to control pollution in a refined manner. Between 2017 and 2022, the average $PM_{2.5}$ concentration values in each district and county were greater than China I standard limit (15 μg/m^3) and much higher than the WHO, 2021AQGs standard limit (15 μg/m^3) (Fig. 4). Among them, the concentration values in Hechuan District, Qijiang District, Bishan District and Rongchang District are all greater than 40 μg/m^3. In addition, the O_3 concentration values in all districts and counties are also higher than China I (100 μg/m^3), and the values in Shapingba District, Jiangjin District and Bishan District exceed the national Grade II standard limit (≤160 μg/m^3). Chongqing is an industrial and transportation hub city located in western China with a high urbanization rate. Urbanization affects the concentration of air pollutants by changing air pollutant emissions, urban form, changes in underlying surfaces, and anthropogenic heat release (Ren & Matsumoto, 2020). Relevant studies also show that areas with concentrated populations and higher GDP have higher concentrations of air pollutants (Huang et al., 2023; Jin et al., 2022; Yang et al., 2023). For example, Yang et al. (2017) explored 30 cities in China through a regression model and found that GDP per capita has a negative impact on SO_2. Fu and LI (2020) combined national-level data and spatial econometric models and found a positive relationship between per capita GDP and $PM_{2.5}$ concentration. The high-value areas of Chongqing's population and GDP from 2017 to 2022 are mainly concentrated in the city proper of Chongqing, with the highest values in Yubei District and the lowest values in Chengkou County (Fig. 5). This also shows that the pollution situation in the city proper of Chongqing is more serious than that of the other two clusters.

3.1.2 Daily Variation Characteristics

Clarifying the spatiotemporal distribution pattern of air pollution is the basis and key issue of air pollution research. Mastering the temporal changes of urban air pollutants can better grasp and optimize regional environmental air quality as a whole. It can be clearly seen from Fig. 6 that the daily concentration of $PM_{2.5}$ fluctuated every year from 2017 to 2022, and decreased significantly. However, the overall risk of

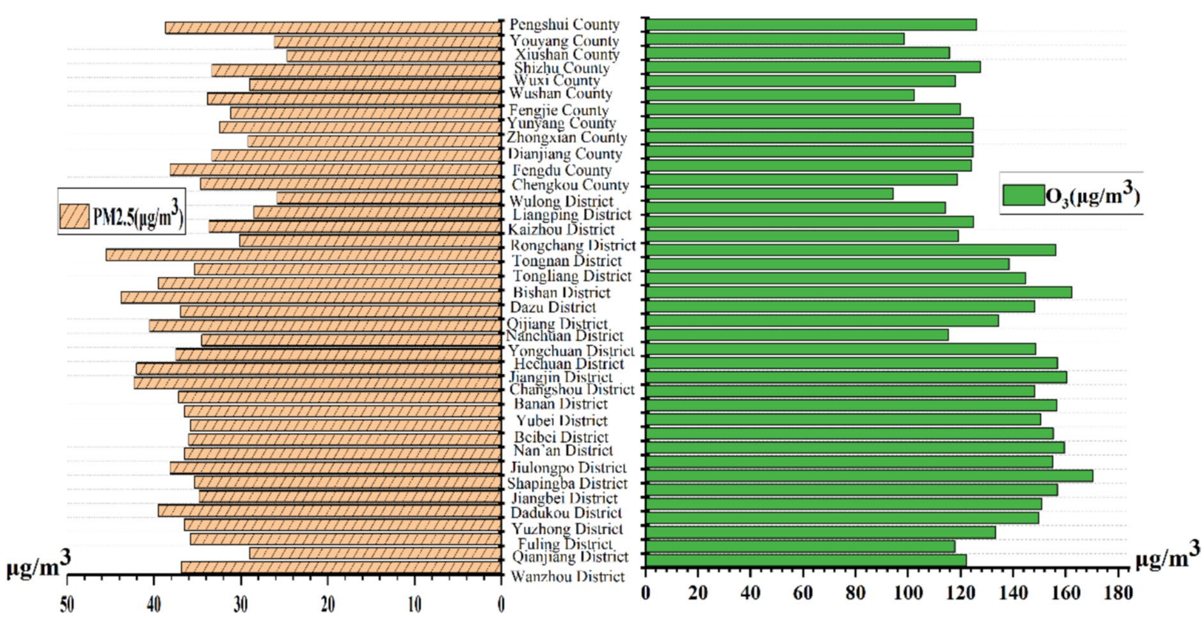

Fig. 4 The Concentration characteristics of $PM_{2.5}$ and O_3 in 2017 to 2022

$PM_{2.5}$ exposure remains large, and anthropogenic emissions remain high. The daily average value in 2017 is higher than that in other years, with higher values in December and January-February (winter), and lower values in June-August (summer). The annual average values from 2017 to 2022 are 43.79μg/m^3, 37.23μg/m^3, 31.98μg/m^3, 38.25μg/m^3, 34.43μg/m^3, 30.96μg/m^3 respectively, with the maximum values appearing in January and December. This shows that $PM_{2.5}$ needs to be controlled especially in autumn and winter. From 2017 to 2022, $PM_{2.5}$ pollution concentration levels are dominated by Excellent and good levels every year, and show an upward trend, with the largest in 2022 (66.3%) (Table 3). In addition, mild pollution and moderate pollution accounted for the largest proportion in 2017 (12.5%), followed by 2021 (8.0%). Existing research has indicated that motor vehicle emissions and catering cooking emissions are primary sources of particulate pollutants in Chongqing (Zhang et al., 2017; Zhou et al., 2019). In 2020, the proportion was the lowest at 3.8%, which is closely related to the relevant lockdown measures during the COVID-19 epidemic, such as the reduction of emissions from factories and transportation (LI et al., 2023; Mi et al., 2019).

It can be seen from Fig. 7 that during the period from 2017 to 2022, the daily changes in O_3 showed a fluctuating increase in peak concentration from January to August, and a fluctuating downward trend from September to December. Generally speaking, O_3 concentration is lower in January-February and December (winter), and higher in May-August (spring and summer). O_3 is generated from nitrogen oxides and volatile organic compounds through a series of complex photochemical reactions under the irradiation of solar ultraviolet (UV) radiation. Chongqing is characterized by long hours of sunshine, strong solar radiation, and high temperatures in summer, which not only accelerate chemical reactions but also increase the volatilization of VOCs. Consequently, the rate and concentration of ozone formation are much higher than in other seasons. However, the "titration effect" of ozone is more pronounced in winter. Near-surface NO concentrations are relatively high in winter, and NO reacts with ozone ($O_3 + NO \rightarrow NO_2 + O_2$), consuming ozone. In addition, the "stable weather" and "valley winds" formed by unique topography also contribute to the increased concentration of pollutants (Li et al, 2021a; Liao et al, 2018). Therefore, the key to preventing and controlling ozone pollution in summer lies in the coordinated reduction of NOx and VOCs precursors. At the same time, it is also necessary to pay attention to the forecasting and early warning of unfavorable meteorological conditions.

In addition, it is worth noting that compared with the $PM_{2.5}$ change trend, the O_3 concentration does not show a downward trend year by year. The proportion of mild pollution in 2021 and 2022 shows

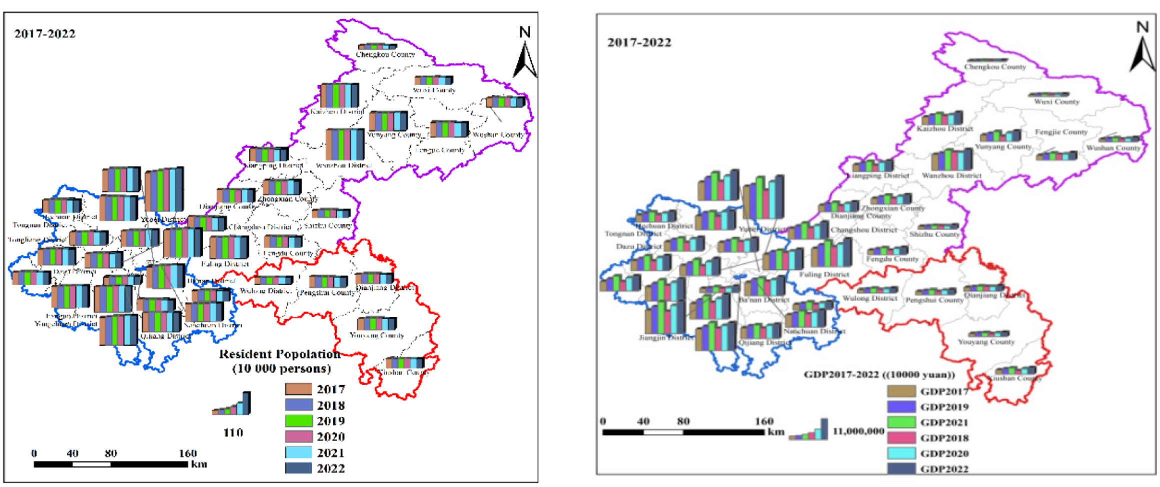

(a) Population distribution

(b) GDP distribution

Fig. 5 Distribution of population and GDP by district and county

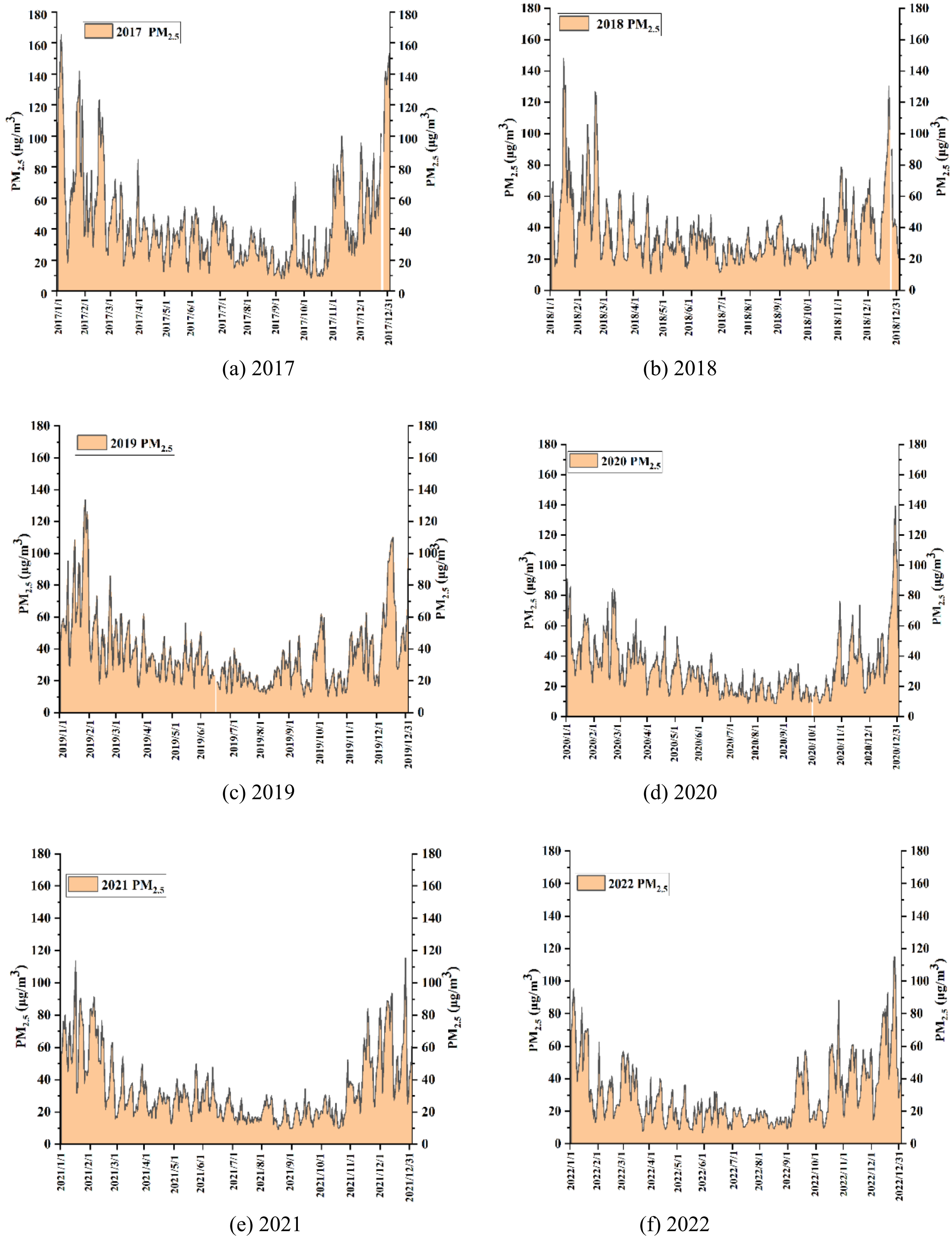

Fig. 6 Daily variation trend of $PM_{2.5}$ concentration

Table 3 $PM_{2.5}$ pollution concentration levels

Grades	$PM_{2.5}$ pollution concentration	2017	2018	2019	2020	2021	2022
Excellent	≤ 35 μg/m^3	48.48%(176 days)	58.7%(214 days)	58%(211 days)	66.4%(243 days)	64.9% (237 days)	66.30% (242 days)
Good	35.01–75.00 μg/m^3	38.22%(139 days)	35.3%(129 days)	36.3%(132 days)	29.8%(109 days)	27.1%(99 days)	29.3%(107 days)
Mild pollution	75.01–115 μg/m^3	8%(29 days)	4.1% (15 days)	4.9%(18 days)	3.3%(12 days)	7.8%(28 days)	4.2%(15 days)
Moderate pollution	115.01–150 μg/m^3	4.5%(16 days)	1.6%(6 days)	0.8%(3 days)	0.5%(2 days)	0.2%(1 day)	0.2%(1 day)
Heavy pollution	150.01–250.01 μg/m^3	0.8% (3 days)	0	0	0	0	0
Severely pollution	≥250μg/m^3	0	0	0	0	0	0

an increasing trend compared with other years, reaching 5.2% in 2022 (Table S3). There were 147 days in 2022 with concentration values higher than 160 μg/m^3. Although the traffic volume and industrial activity level decreased significantly during the COVID-19 epidemic, and the emission of air pollutants decreased significantly, the O_3 concentration showed a recovery trend to varying degrees (Deng et al., 2022a, b); LI et al., 2023; Zeng & Bao, 2021). In 2020, especially during the period of strict epidemic control, traffic volume decreased sharply and some factories stopped operating, resulting in a rapid decline in NOx emissions. Meanwhile, VOCs from industrial and transportation sources have decreased, and the overall reduction in VOCs is less than that of NOx. This will lead to a shift in the "titration effect" of ozone formation mechanisms, meaning that high concentrations of NO will consume ozone. In 2021, with the normalization of epidemic control, social and economic activities resumed. Due to the rapid recovery of industrial production and road traffic, NOx emissions rebounded rapidly, and the recovery rate was faster than that of VOCs. When NOx emissions recover while VOCs control fails to be strengthened simultaneously, the relatively excessive VOCs, under sufficient sunlight, efficiently generate ozone. The changes in O_3 concentration during the COVID-19 pandemic in Chongqing reveal the complexity of O_3 pollution prevention and control.

Based on the national overall goal of air pollution prevention and control, Chongqing has also actively proposed many prevention and control measures to improve air quality and promote the realization of the regional "double carbon" goal. For example, "Chongqing Autumn and Winter Air Pollution Prevention and Control Actions" were promulgated in 2017; and in 2018 Promulgated "Chongqing City's Implementation Plan for Pollution Prevention and Control (2018-2020)" (Gou & Liu, 2022; Ji et al., 2019; Maji et al., 2018). Through this series of measures, the air pollution situation in Chongqing has been significantly improved, especially $PM_{2.5}$ pollution has been effectively improved. However, O_3 pollution is still serious. Therefore, O_3 emission reduction must be based on local atmospheric chemical conditions (whether it is a VOCs control area or a NOx control area), and precise and coordinated NOx and VOCs emission reduction strategies must be formulated.

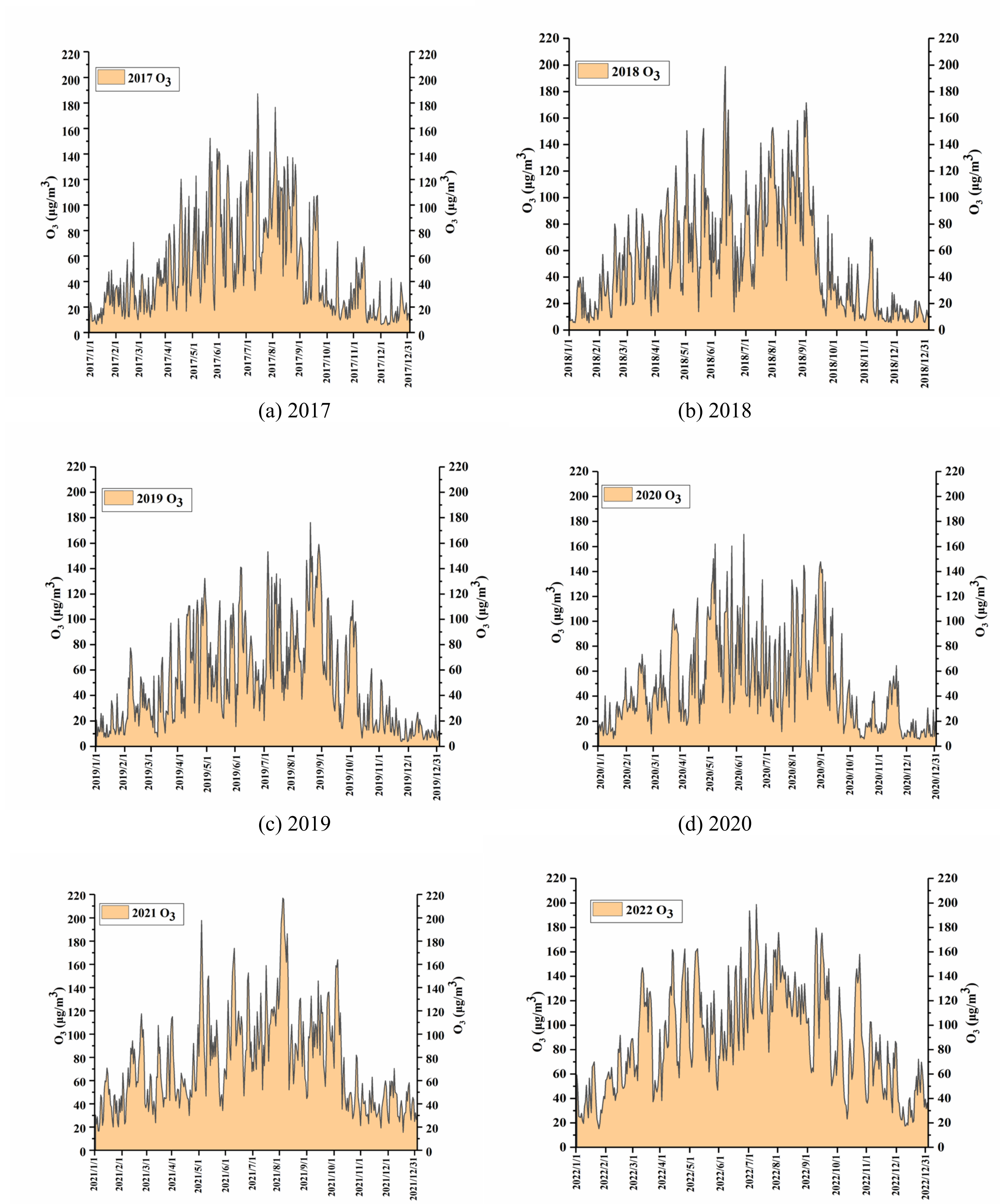

(a) 2017 (b) 2018

(c) 2019 (d) 2020

(e) 2021 (f) 2022

Fig. 7 Daily variation trend of O_3 concentration

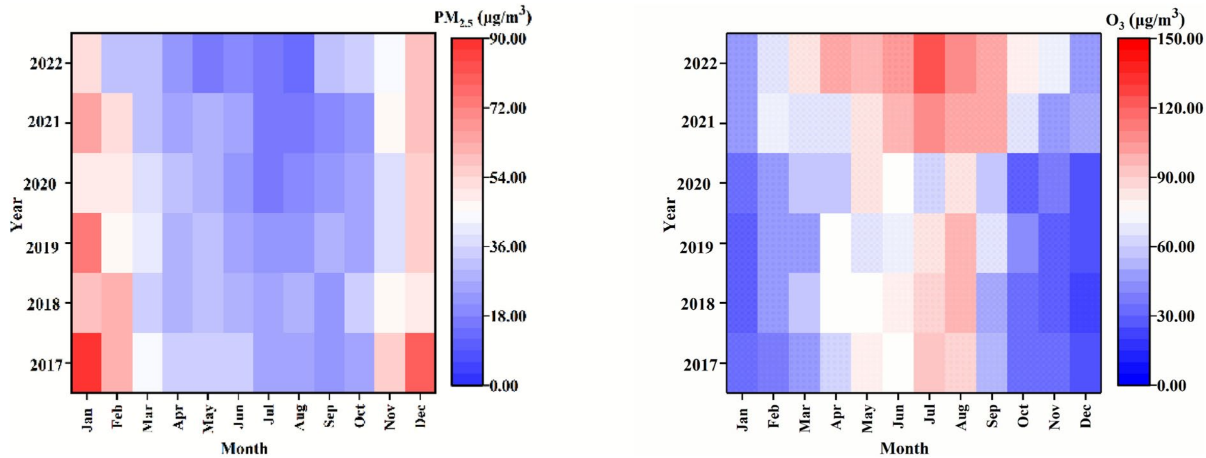

Fig. 8 Heat map of monthly changes of $PM_{2.5}$ and O_3 (2017 - 2022)

3.1.3 Monthly Variation Characteristics

It can be seen from Fig. 8 that from 2017 to 2022, the high concentration values of $PM_{2.5}$ are mainly concentrated in January, February and December, and the high concentration values of O_3 are mainly concentrated in May to August. This is basically consistent with the analysis results of diurnal changes of $PM_{2.5}$ and O_3 (Fig. 6 and Fig. 7). That is, $PM_{2.5}$ has the highest value in winter and O_3 has the highest value in summer. The enhanced oxidation of the atmosphere in winter promotes $PM_{2.5}$ pollution (Huang et al., 2023; Zhou et al., 2019). In addition, the figure also shows that the monthly concentration value of $PM_{2.5}$ decreased year by year from 2017 to 2022, indicating that $PM_{2.5}$ pollution has been effectively improved. This also demonstrates the significant effectiveness of Chongqing's energy and industrial restructuring and in-depth treatment of mobile source pollution, including end-of-pipe treatment and source substitution measures. On the contrary, O_3 concentration shows a certain upward trend, especially in summer. The O_3 concentration value in the summer of 2022 is higher than that of other years, which shows that O_3 pollution has not been significantly alleviated in recent years. O_3 is a typical secondary pollutant, and its relationship with NOx and VOCs is not linear. High summer temperatures accelerate photochemical reaction rates, leading to increased ozone concentrations. In addition, $PM_{2.5}$ (aerosols) scatters and absorbs solar radiation. When the concentration of $PM_{2.5}$ decreases significantly, the solar radiation reaching the ground increases, thereby improving the efficiency of photochemical reactions. In the past 40 years, rising temperatures and falling humidity in China have aggravated O_3 pollution, and regional transmission caused by abnormal circulation is the dominant factor leading to extreme O_3 pollution in the SCB. O_3 pollution mainly involves the complex chemical coupling between the emission of precursors and other pollutants and the influence of meteorological factors (Liu et al., 2021, 2022; Si et al., 2024). Therefore, the control of O_3 pollution needs to further consider the reduction of precursors and the influence of meteorological factors. Furthermore, developing differentiated and coordinated emission reduction plans is also crucial.

3.1.4 Correlation Analysis Between $PM_{2.5}$ and O_3

Understanding the relationship between $PM_{2.5}$ and O_3 is the basis for implementing coordinated control and the key to winning the battle to defend the blue sky. The correlation scatter plot shows that when the $PM_{2.5}$ concentration increases, the O_3 concentration tends to decrease (Fig. 9). R is all negative from 2017 to 2022, indicating that $PM_{2.5}$ and O_3 are negatively correlated ($R<0$). The degree of dispersion of points is large, and an increase in the concentration of one will cause a decrease in the concentration of the other. This also reveals the inherent antagonistic mechanism of complex air pollution in Chongqing.

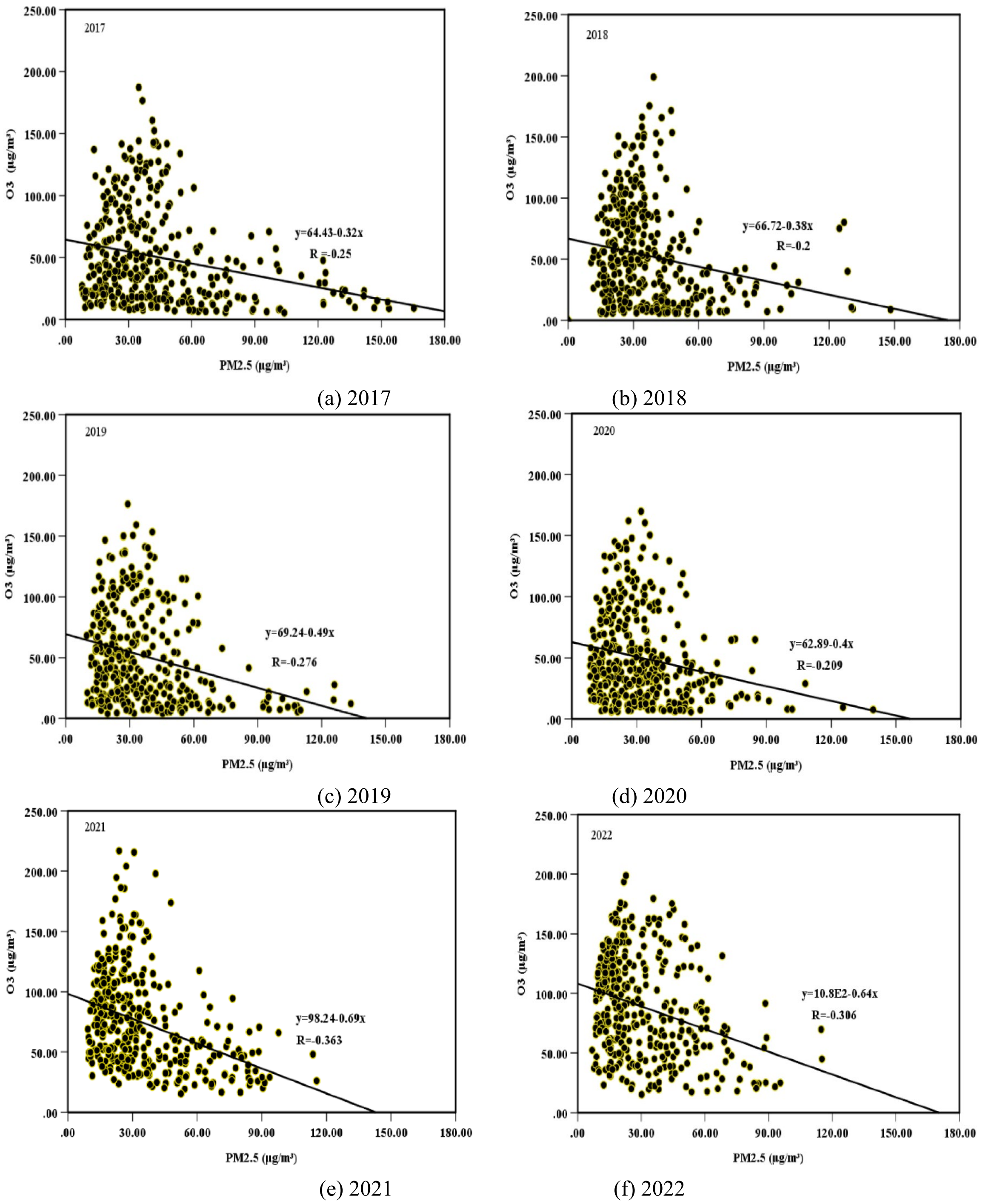

Fig. 9 Scatter plot of the relationship between $PM_{2.5}$ and O_3

Overall, the complex relationship between $PM_{2.5}$ and O_3 is influenced by a combination of factors. $PM_{2.5}$ and O_3 interact with each other through aerosol chemical absorption and scattering, heterogeneous reactions, and changes in atmospheric oxidation (Chu et al., 2024; Ma et al., 2023). The decrease in $PM_{2.5}$

concentration leads to a weakening of the scavenging effect of nitrogen oxides and HO_2, which in turn leads to an increase in O_3 and affects the sensitivity of ozone generation (Deng et al., 2022a, b); Mi et al., 2019). Furthermore, Chongqing's unique topography and meteorological conditions exacerbated this negative correlation. However, relevant scholars have suggested that the root cause of China's O_3 pollution in recent years is mainly caused by excessive and concentrated emissions of two precursor pollutants, NOx and VOCs (Lee et al., 2023; Tan et al., 2018). Therefore, strengthening the synergistic reduction of common precursors (VOCs and NO_x) of $PM_{2.5}$ and O_3 is an effective way to achieve simultaneous reduction of both. Chongqing should promote the transformation of its steel industry towards ultra-low emissions and thoroughly address pollution in industries such as cement, coking, and glass. At the same time, it should strengthen pollution control for motor vehicles. In addition, policy measures should be tailored to the season, with a focus on controlling O_3 precursors in summer and primary particulate matter in winter.

3.2 Spatial Heterogeneity of Pollutants in Districts and Counties

3.2.1 Spatiotemporal Distribution of $PM_{2.5}$ Pollutants

Exploring the spatial distribution characteristics of air pollutant concentrations in megacities will help improve regional air quality, improve urban life quality, and provide a basis for traceability and predictions of pollutants. Figure 10 shows that the $PM_{2.5}$ concentration value in the entire region of Chongqing shows a downward trend from 2017 to 2022. In particular, the $PM_{2.5}$ concentration in the city proper of Chongqing has improved significantly. The $PM_{2.5}$ pollution concentration in 2017 was more serious than in other years, with Hechuan District, Rongchang District and Shapingba having the highest concentration values. High concentration values of $PM_{2.5}$ in the city cluster of three gorges reservoir area in northeast Chongqing are mainly concentrated in Fengdu County and Changshou County. In addition, the concentration values of $PM_{2.5}$ in the city cluster of Wuling Mountain area in south eastern Chongqing are lower than China I standard limit (35μg/m^3). Compared with 2017, the $PM_{2.5}$ concentration value in 2018 improved significantly in the city proper of Chongqing, but the value in Rongchang District was still the largest. In 2019, the pollution concentration in about 80% of the city proper of Chongqing was between 34μg/m^3 and 41μg/m^3. In 2020, the $PM_{2.5}$ concentration improved significantly, with about 90% of regional concentration values below 34 μg/m^3. In 2020, due to strict epidemic control measures, the number of motor vehicles decreased significantly, and industrial and construction activities weakened, resulting in a temporary reduction in industrial emissions and dust emissions. However, compared with 2020, $PM_{2.5}$ pollution areas in 2021 have a certain expansion trend in the city proper of Chongqing, and the concentration values in some areas show an upward trend. The $PM_{2.5}$ is affected by many factors, among which emissions are the main cause, atmospheric physical and chemical processes are internal factors, and meteorological conditions are external factors. The rebound and expansion of $PM_{2.5}$ pollution in 2021 was a combined result of economic "recovery growth" and "unfavorable meteorological catalysts". This shows that fundamental improvement in air quality depends on long-term structural emission reductions, and improvements brought about by short-term external shocks (such as the pandemic) are unsustainable.

3.2.2 Spatiotemporal Distribution of O_3 Pollutants

Exploring the spatial pollution characteristics of $PM_{2.5}$ and O_3 is a prerequisite for achieving coordinated control. It is obvious that there are significant differences in the spatial distribution of O_3 concentration between districts and counties in the same year (Fig. 11). In addition, the high-value areas of O_3 during the study period were observed in the city proper of Chongqing. From 2017 to 2019, more than 90% of districts and counties in Chongqing had O_3 concentrations higher than 100 μg/m^3. The highest values in Jiangjin District, Hechuan District and Yongchuan District appeared in 2017, 2018 and 2019 respectively. Compared with 2017-2019, the distribution range of high O_3 concentration areas shows a shrinking trend in 2020-2021. Overall O_3 pollution has been reduced and controlled to some extent. This may be closely related to the lockdown measures taken during the epidemic (Bai et al., 2022a, b); Zhang et al., 2022). However,

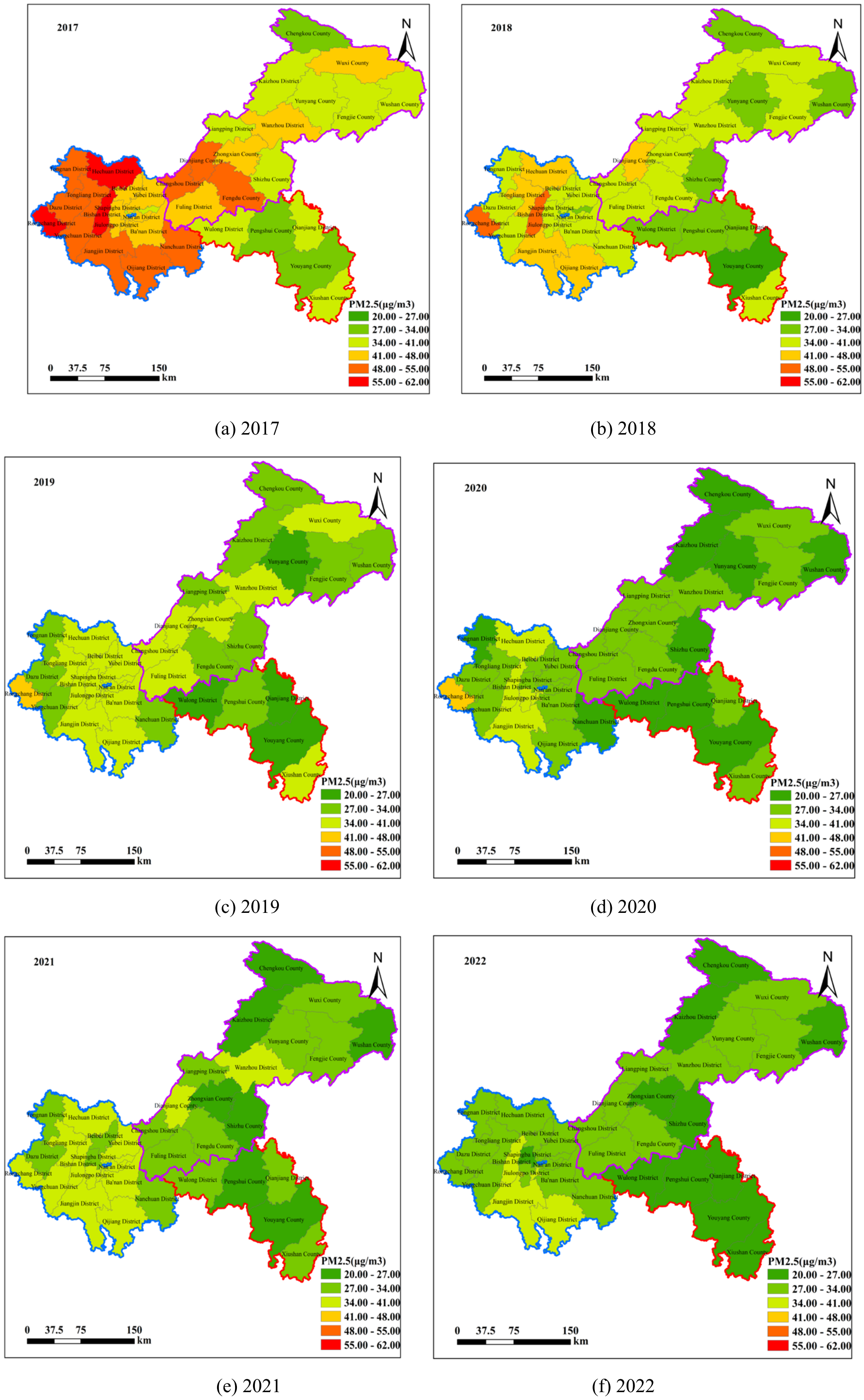

Fig. 10 Spatiotemporal distribution of $PM_{2.5}$ (2017-2022)

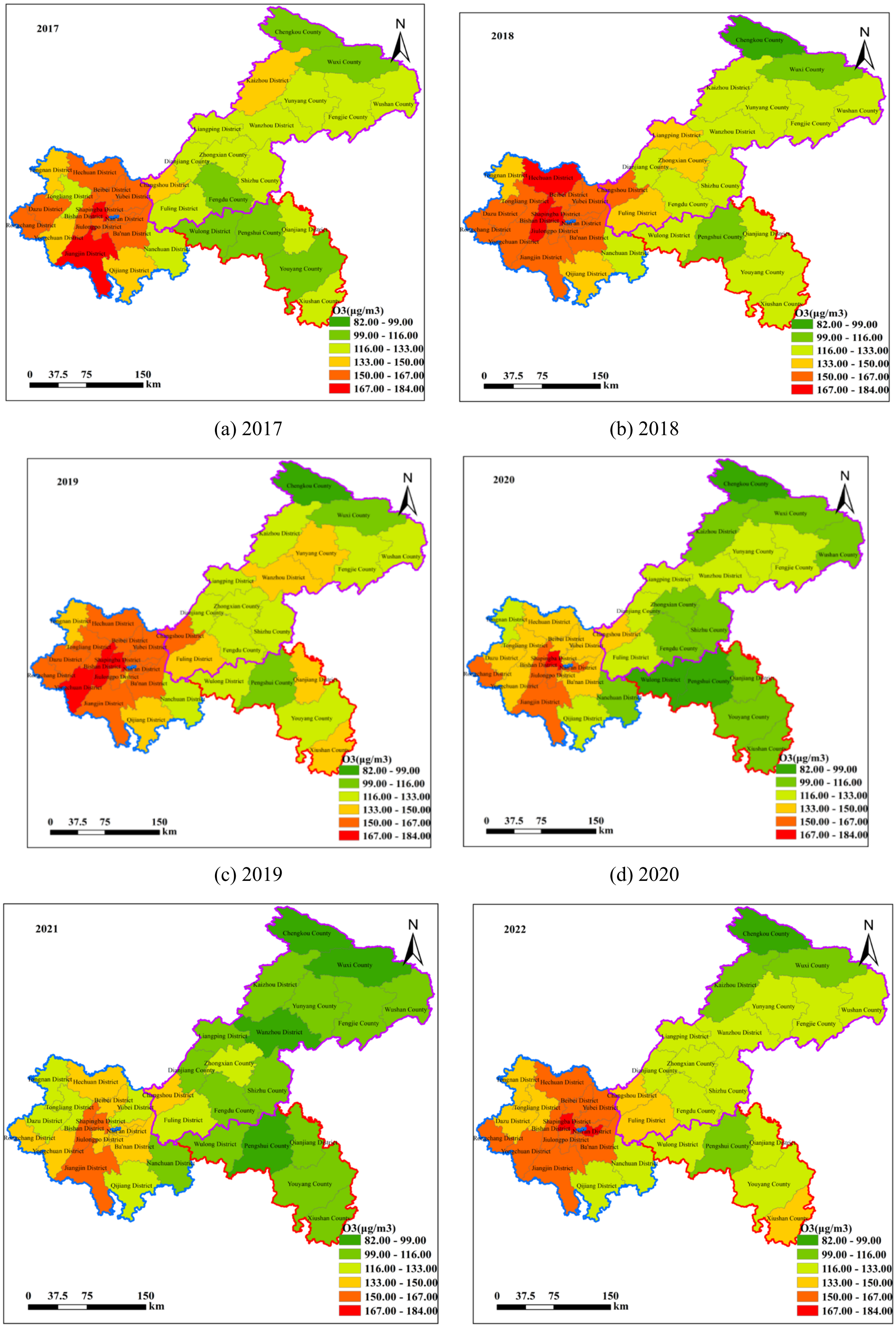

(a) 2017 (b) 2018

(c) 2019 (d) 2020

(e) 2021 (f) 2022

Fig. 11 Spatiotemporal distribution of O_3 (2017-2022) the O_3 high concentration value area in 2022 shows a certain expansion trend compared with 2019-2021. This is mainly due to the increase in industrial production and human activities after the epidemic, and also reflects the urgency of O_3 pollution prevention and control in Chongqing. Related studies have revealed the complex nonlinear relationship between O_3 and its precursors (Chen et al., 2022; Liu et al., 2022). Controlling the emission of a single precursor may not effectively reduce O_3 concentration, and may even cause O_3 concentration to rise instead of falling. Therefore, to better achieve precise control of O_3 pollution, it is necessary to further identify the sensitivity of O_3 generation to precursor VOCs and NOx, and clarify the regional characteristic relationship between O_3 pollution, precursor emissions and meteorology.

3.3 The Spatial Autocorrelation of $PM_{2.5}$ and O_3

3.3.1 Moran's I Analysis of $PM_{2.5}$

The emission and diffusion of atmospheric pollutants involve complex spatiotemporal and geographical spatial processes, showing certain spatial correlation (Ren & Matsumoto, 2020). In order to quantitatively measure the spatial dependence of air pollutant distribution in neighboring areas, the global Moran index was calculated based on the geographical distance weight matrix. Simultaneously, this index was used to characterize the spatial autocorrelation of $PM_{2.5}$ in Chongqing from 2017 to 2022. Since this study primarily aims to preliminarily identify potential risk areas for pollutants, the p-value is derived from a permutation test. Furthermore, the study uses Chongqing's urban districts and counties as units, which have a limited number of spatial units. Therefore, a 90% significance level ($p < 0.1$) was chosen. Overall, the global Moran's I index passed the significance test every year during the study period ($p < 0.1$). The Z value is greater than 2.58, indicating that the $PM_{2.5}$ concentration in Chongqing shows significant spatial autocorrelation and aggregation characteristics at a 90% confidence level. In addition, Table 4 shows that Moran's I value in Chongqing from 2017 to 2022 are all higher than 0. This indicates that the geographical distribution of $PM_{2.5}$ within the study period exhibits positive spatial autocorrelation.

Moreover, the $PM_{2.5}$ pollutant status of each district and county is significantly affected by similar pollution in neighboring districts and counties. Among them, the Moran's I in 2021 is the largest, indicating a high degree of spatial aggregation, while the Moran's I index in 2019 is the lowest. It is obvious that the Moran's I of $PM_{2.5}$ concentration decreased significantly from 2017 to 2020, which were 0.407, 0.396, 0.283 and 0.267, respectively. It can also be seen from Fig. 12 that scattered points are mainly distributed in the first and third quadrants. That is, there are obvious HH aggregation and LL agglomeration in the $PM_{2.5}$ concentration distribution. This shows that districts and counties with high (low) concentrations of $PM_{2.5}$ are surrounded by districts and counties with high (low) concentrations. Furthermore, this also demonstrates that pollution is not randomly distributed, but rather exhibits a significant spatial clustering pattern of "high concentrations remaining high and low concentrations remaining low." In other words, pollution problems have strong regional and contiguous characteristics. Therefore, prevention and control strategies must shift from "targeting isolated point sources" to a systemic approach that "targets the entire spatial region and inter-regional relationships (Xu et al., 2021; Yu et al., 2019; Zhang et al., 2018)."

Table 4 Moran's I statistics for $PM_{2.5}$ from 2017 to 2022

Year	Morans'I	Z-score	P-value
2017	0.407	6.36	0.069
2018	0.396	6.18	0.069
2019	0.283	4.58	0.068
2020	0.267	4.42	0.067
2021	0.546	8.60	0.067
2022	0.506	7.94	0.067

3.3.2 Moran's I Analysis of O_3

Global Moran's I can clarify the distribution pattern of O_3 concentration in the study area. As can be seen from Table S4, the Moran's I value of O_3 from 2017 to 2022 are all positive, and the Z value is also greater than 2.58. It shows that O_3 emission is statistically significant at a confidence level of 90% ($p<0.1$) and the emission distribution has spatial positive aggregation characteristics. Over the six years, Moran's I value mostly fluctuated between 0.64 and 0.77. This indicates that the spatial correlation of O_3 concentrations across different regions and counties did not change significantly between 2017 and 2022. And the Moran's I value of O_3 concentration is higher than 0.5, which also indicates high spatial overflow. Overall, the O_3 spatial autocorrelation level showed an upward trend during the study period, indicating that spatial autocorrelation was enhanced. The Moran's I scatter plot further confirmed that there is a significant positive spatial autocorrelation in the annual average O_3 concentration from 2017 to 2022. This also proves that areas with high (low) O_3 concentrations are surrounded by other areas with high (low) O_3 concentrations (Fig. 13). In addition, the points in the first and third quadrants are distributed further than the points in the second and fourth quadrants. This further illustrates the spatial imbalance and positive spatial correlation characteristics of the O_3 concentration distribution. Especially in the first and third quadrants, there are obviously more points than in the second and fourth quadrants, and they show a clustered distribution around the origin. It shows that there are more HH and LL agglomeration areas. That is, areas with higher or lower O_3 emission concentrations are more likely to be spatially agglomerated. This also indicates that O_3 pollution has regional pollution sources or areas with significant pollution diffusion effects, as well as "clean cold spots". Therefore, pollution control measures must emphasize regional coordination and implement "precise policies based on regional classification." Furthermore, attention must also be paid to "spatial layout and structural optimization."

3.4 Spatial Aggregation and Significance Analysis

3.4.1 Spatial Aggregation Characteristics

Spatial Aggregation Characteristics of $PM_{2.5}$ There may be certain differences in spatial autocorrelation levels between adjacent districts and counties, but the global Moran scatter plot can only represent the spatial aggregation characteristics of pollutants and cannot provide any regional significance test results. The LISA cluster map in local Moran's I index analysis can well discover the potential changing trends of air pollution and severely polluted areas (Dong et al., 2019). From Fig. 14, it can be found that the spatial distribution of $PM_{2.5}$ shows a pattern of high in the west and low in the east, with high value areas (HH) mainly distributed in the city proper of Chongqing. Moreover, its distribution characteristics showed annual differences during the study period. During 2017-2022, the number of districts and counties belonging to the HH and LL clusters were 15 (39.5%), 14 (36.8%), 8 (21.1%), 10 (26.3%), 27 (71.1%) and 21 (55.3%), respectively. This further demonstrates the spatial autocorrelation of $PM_{2.5}$ concentration in Chongqing (Table 5). Among them, the HH aggregation area was the smallest in 2019, and the distribution ranges of both HH and LL aggregation areas were the largest in 2021. This indicates that the positive spatial correlation characteristics of $PM_{2.5}$ are the most significant in 2021. In 2017, the HH cluster area was mainly found in the city proper of Chongqing, including Tongnan District, Yongchuan District, Tongliang District, Rongchang District and Dazu District. The spatial clustering analysis in 2018 showed that its distribution characteristics were similar to those in 2017. However, the HH region showed an expanding trend compared to 2017, while the LL clustering region showed a certain shrinking trend. The spatial aggregation distribution pattern of $PM_{2.5}$ in 2019 are obviously different from other years. The distribution range of HH agglomeration areas is small and mainly concentrated in a small number of areas (Jiangjin District, Beibei District, Yubei District). The number of districts and counties with HH clusters in 2020 is the same as that in 2019, but the regions have changed slightly. In 2021, the HH agglomeration area has increased to 16 districts and counties, widely observed in the central city of Chongqing. Compared with 2021, the HH and LL agglomeration areas have shown a certain decrease in 2022, but the distribution area is basically the same as in 2021.

Spatial Aggregation Characteristics of O_3 From the results in Fig. 15, we can have a clear view about the detailed structure of spatial clustering of O_3. Undoubtedly, the agglomeration characteristics of HH and LL are very obvious. That is, a district or county with high or low O_3 values is always surrounded by other areas with higher or lower O_3 concentrations. The number of districts and counties with HH clusters was 16 (42.1%) in 2017, and 17 (44.7%) in 2018-2022. And the number of districts and counties in the LL cluster is 15 in 2021, and 14 (36.8%) in the other years (Table S5). In addition, it is worth noting that the HH cluster area covers the city proper of Chongqing. In contrast, the

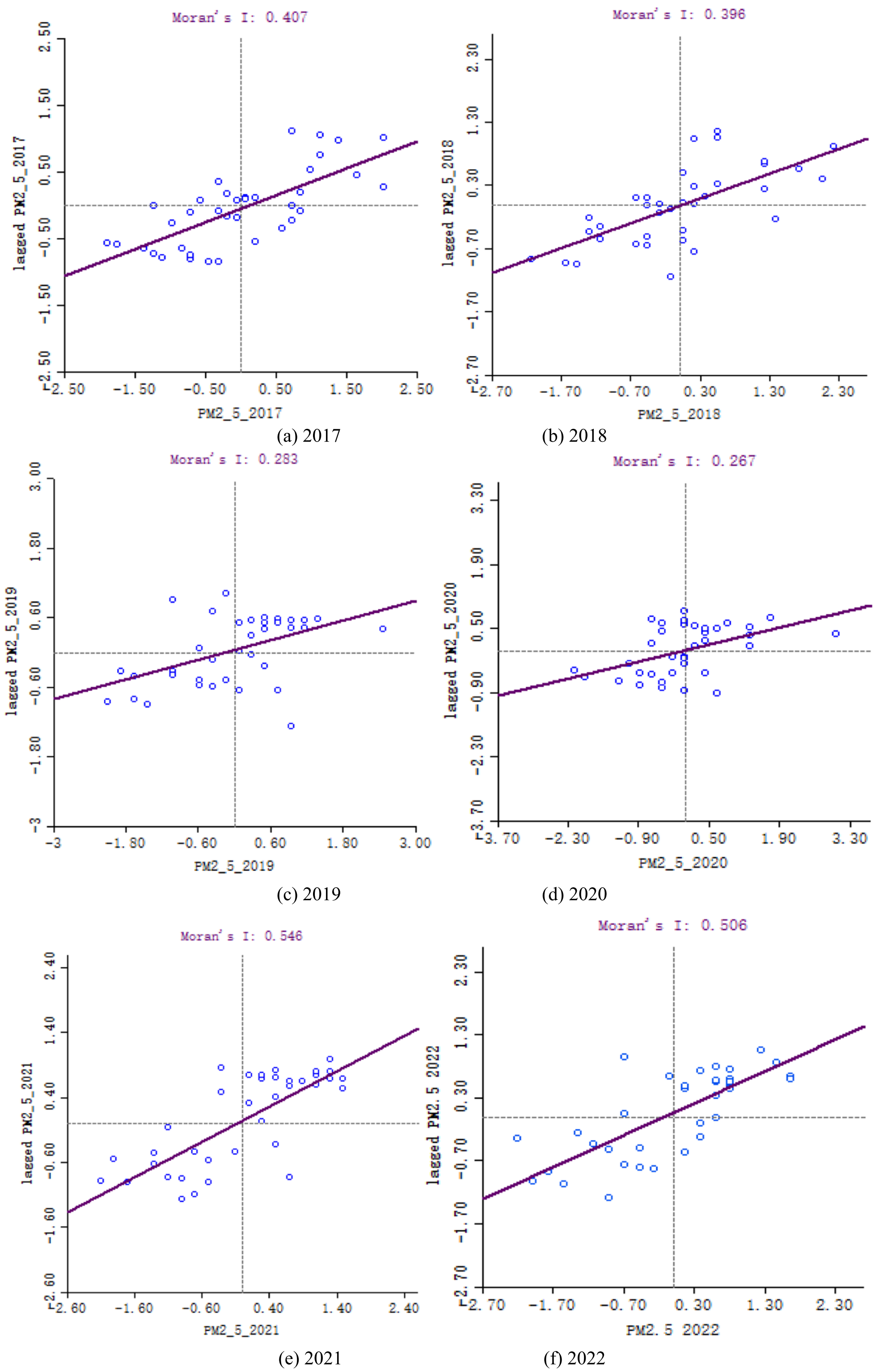

Fig. 12 $PM_{2.5}$ Air Pollution Moran's I Scatter Plots (2017-2022)

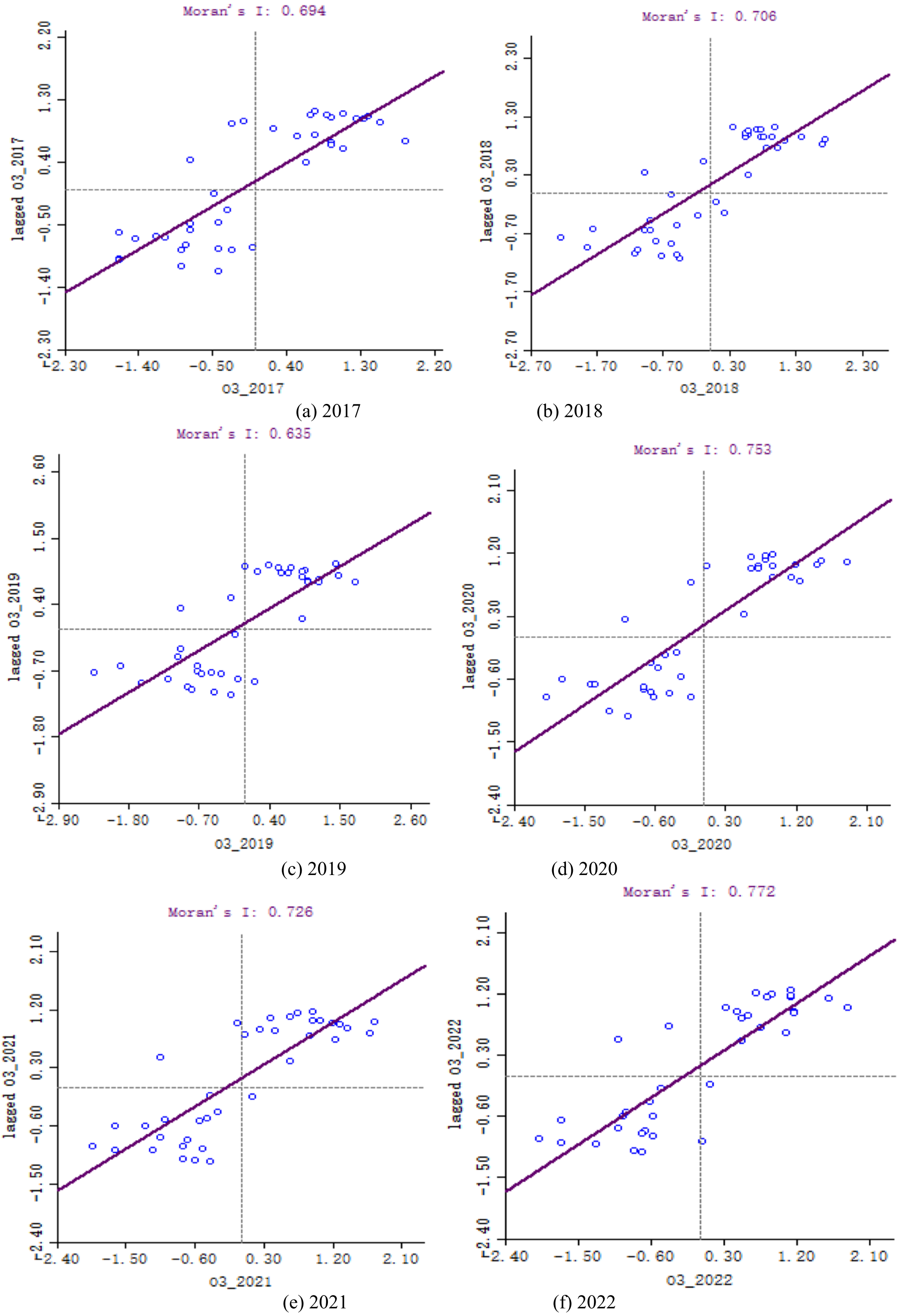

(a) 2017 (b) 2018

(c) 2019 (d) 2020

(e) 2021 (f) 2022

Fig. 13 Moran's I Scatter Plots of O_3 (2017-2022)

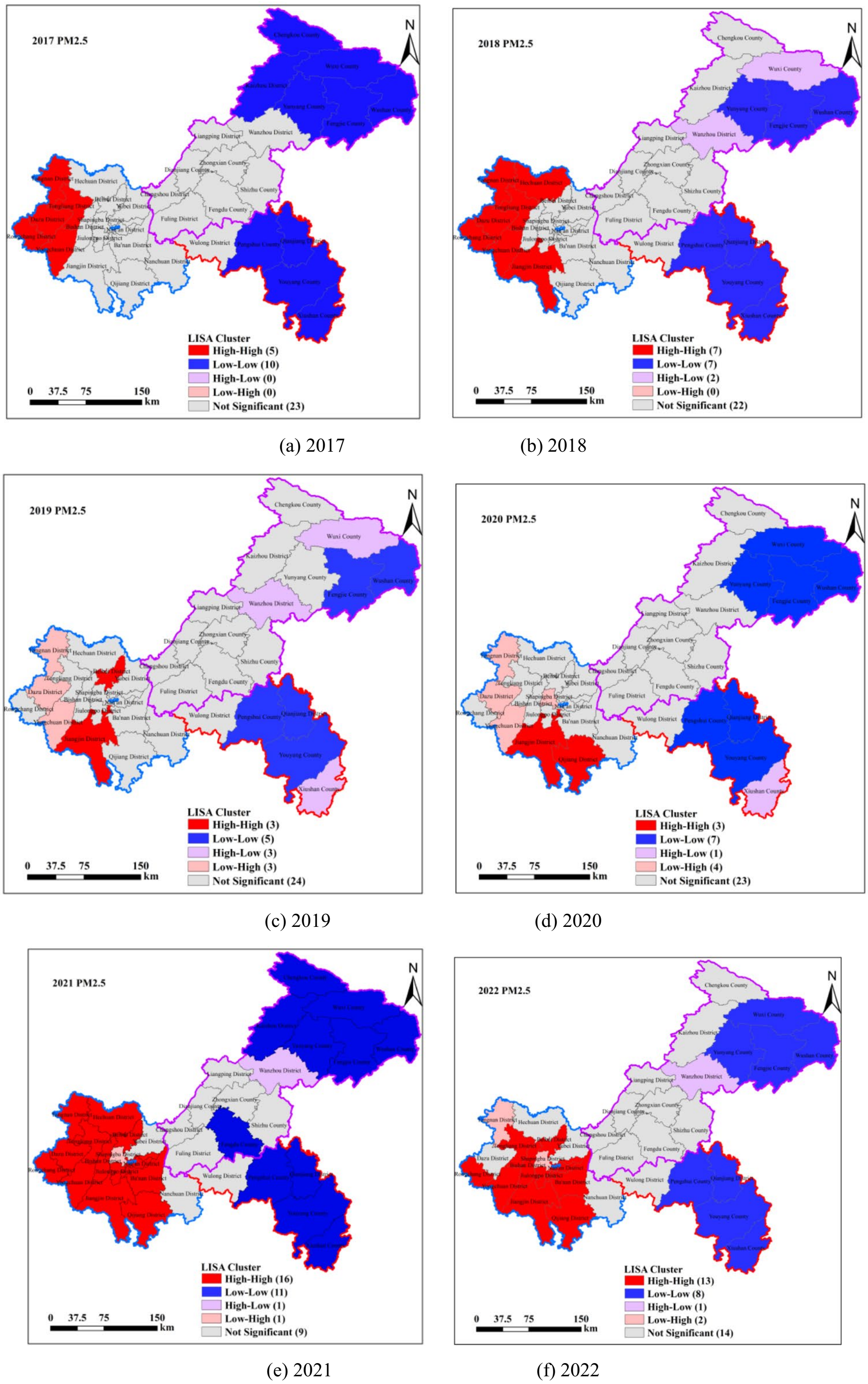

(a) 2017 (b) 2018

(c) 2019 (d) 2020

(e) 2021 (f) 2022

Fig. 14 LISA cluster maps for $PM_{2.5}$ concentration (2017-2022). Note: The number represented the number of corresponding districts and counties districts and counties belonging to the LL cluster type are mainly concentrated in the city cluster of Wuling Mountain area in south eastern Chongqing and the city cluster of three gorges reservoir area in northeast Chongqing. Obviously, the LL agglomeration area accounts for the largest area, followed by the HH area. The HL and LH cluster areas are very small in size, with only a few scattered grids. From a spatiotemporal distribution perspective, the regional distribution characteristics of positive spatial autocorrelation (HH and LL) remained largely consistent throughout the study period. This indicates that O_3 exhibited strong positive spatial correlation in each year. Generally speaking, the spatial aggregation characteristics of O_3 are significantly stronger than that of $PM_{2.5}$. However, the regional distribution of HH aggregation types of O_3 is basically consistent with that of $PM_{2.5}$, both of which are mainly concentrated in the city proper of Chongqing. The rapid development of urbanization in the main urban area coupled with the increase in industrial activities and the number of motor vehicles has jointly led to high $PM_{2.5}$ and O_3 concentrations in this area.

3.4.2 Spatial Significance Characteristics

Spatial Significance Characteristics of $PM_{2.5}$ The z-value and p-value can be used to determine whether to reject the null hypothesis (random distribution) and thus characterize statistical significance. A smaller p-value indicates that it is less likely that the spatial pattern is random (Liu et al., 2022). P<0.1 indicates that the null hypothesis is rejected at the 90% confidence interval, and P>0.1 means there is no spatial autocorrelation in the research object (LI et al., 2017). In addition, when P<0.01, it revealed that the null hypothesis is rejected at the 99% confidence interval. That is, the research object has spatial autocorrelation (LI et al., 2017). LISA significant map can make up for the shortcomings of Moran's scatter plot. The LISA agglomeration diagram can not only clearly display the type of aggregation of observation units, but also present the significance level of local spatial agglomeration around the observation area (Liu et al., 2022; Mi et al., 2021). This makes up for the shortcomings of Moran scatter plots. In order to better understand the spatial clustering of $PM_{2.5}$ concentration in the study area, Figure 16 reports the detailed information on the spatial significance of $PM_{2.5}$ between 2017 and 2022. It is obvious that there are differences in spatial distribution of P values in the study area (2017-2022). The number of districts and counties with P<0.001 in 2021 is significantly higher than in other years, followed by 2022. Overall, the spatial significance characteristics are consistent with the significant clustering regions shown in the clustering diagram, such as high-high (hot spots) and low-low (cold spots). This indicates that these regions (HH and LL) remain significant at the 95% significance level ($p < 0.05$). This means that the spatial distribution of pollutant concentrations exhibits a highly significant clustering pattern. The phenomenon of high-value areas being adjacent to high-value areas and low-value areas being adjacent to low-value areas is not accidental. This result provides spatial statistical evidence for the subsequent implementation of precise environmental control policies based on zoning and classification.

Spatial Significance Characteristics of O_3 Figure 17 can help us better understand the spatial significance structure of O_3 concentration values in Chongqing. Most districts and counties passed the significance test ($p \leq 0.1$) between 2017 and 2022. In addition, the distribution characteristics of the regions with $P < 0.1$ shown in Fig. 17 are consistent with the characteristics of the HH and LL regions shown in Fig. 15. This further indicates that the O_3 distribution in this region remains spatially significant at a 95% significance level ($p < 0.05$). During the study period, the P value of most areas in Chongqing's central urban area was 0.01, and the P value of some areas was 0.001. This indicates that the confidence levels in these areas were 99% and 99.9%, respectively. In addition, the P values in the city cluster of three gorges reservoir area in northeast Chongqing are all lower than 0.1, indicating that this area exhibits spatial autocorrelation at the confidence level of 90%, 95%, and 99.9%. In most areas of the city cluster of Wuling Mountain area in south eastern Chongqing, the P value is less than 0.1. The clustered distribution with a P value of 0.001 mainly occurred in the southeastern part of the Wuling Mountain urban agglomeration (2017, 2020) and the northeastern part of the Three Gorges Reservoir urban agglomeration (2021-2022).

Table 5 Spatial Correlation of $PM_{2.5}$ pollutant

Year	Quadrant	Spatial Correlation	Number	Rate	Details of districts and counties
2017	Quadrant 1	HH	5	13.2%	The city proper of Chongqing: Tongnan District, Tongliang District, Dazu District, Rongchang District, Yongchuan District.
	Quadrant 3	LL	10	26.3%	The city cluster of Wuling Mountain area in south eastern Chongqing and the city cluster of three gorges reservoir area in northeast Chongqing: Chengkou Country, Wuxi Country, Wushan Country, Fengjie Country, Yunyang Country, Kaizhou District, Qijiang District, Youyang District, Pengshui Country, Xiushan Country.
	Quadrant 2	LH	0	0	---
	Quadrant 4	HL	0	0	---
	---	NS	23	60.5%	The city proper of Chongqing and the city cluster of Wuling Mountain area in south eastern Chongqing.
2018	Quadrant 1	HH	7	18.4%	The city proper of Chongqing: Tongnan District, Tongliang District, Dazu District, Rongchang District, Yongchuan District, Jiangjin District, Hechuan District.
	Quadrant 3	LL	7	18.4%	The city cluster of Wuling Mountain area in south eastern Chongqing and the city cluster of three gorges reservoir area in northeast Chongqing: Qijiang District, Wushan Country, Fengjie Country, Yunyang Country, Youyang District, Pengshui Country, Xiushan Country.
	Quadrant 2	LH	0	0	--
	Quadrant 4	HL	2	5.2%	The city cluster of three gorges reservoir area in northeast Chongqing: Wuxi Country, Wanzhou District.
	---	NS	22	57.9%	The city proper of Chongqing and the city cluster of three gorges reservoir area in northeast Chongqing.
2019	Quadrant 1	HH	3	7.9%	The city proper of Chongqing: Jiangjin District, Beibei District, Yubei District.
	Quadrant 3	LL	5	13.2%	The city cluster of Wuling Mountain area in south eastern Chongqing and the city cluster of three gorges reservoir area in northeast Chongqing: Qijiang District, Wushan Country, Fengjie Country, Youyang District, Pengshui Country.
	Quadrant 2	LH	3	7.9%	The city cluster of three gorges reservoir area in northeast Chongqing: Tongnan District, Dazu District, Yongchuan District.
	Quadrant 4	HL	3	7.9%	The city cluster of Wuling Mountain area in south eastern Chongqing and the city cluster of three gorges reservoir area in northeast Chongqing: Wuxi Country, Wanzhou District, Xiushan Country.
	---	NS	24	63.2%	The city proper of Chongqing and the city cluster of three gorges reservoir area in northeast Chongqing.
2020	Quadrant 1	HH	3	7.9%	The city cluster of three gorges reservoir area in northeast Chongqing: Jiangjin District, Qijiang District, Jiulongpo District.
	Quadrant 3	LL	7	18.4%	The city cluster of Wuling Mountain area in south eastern Chongqing and the city cluster of three gorges reservoir area in northeast Chongqing: Wushan Country, Fengjie Country, Yunyang Country, Wuxi Country, Pengshui Country, Youyang Country, Qijiang District.
	Quadrant 2	LH	4	10.5%	The city proper of Chongqing: Tongnan District, Dazu District, Yongchuan District, Shapingba District.
	Quadrant 4	HL	1	2.6%	The city cluster of Wuling Mountain area in south eastern Chongqing: Xiushan Country.
	---	NS	23	60.5%	The city proper of Chongqing and the city cluster of three gorges reservoir area in northeast Chongqing.

Table 5 (continued)

Year	Quadrant	Spatial Correlation	Number	Rate	Details of districts and counties
2021	Quadrant 1	HH	16	42.1%	The city proper of Chongqing: Tongnan District, Tongliang District, Dazu District, Rongchang District, Yongchuan District, Jiangjin District, Hechuan District, Qijiang District, Ba'nan District, Nan'an District, Jiulongpo District, Bishan District, Beibei District, Shapingba District, Yuzhong District, Dadukou District.
	Quadrant 3	LL	11	28.9%	The city cluster of Wuling Mountain area in south eastern Chongqing and the city cluster of three gorges reservoir area in northeast Chongqing: Chengkou Country, Wuxi Country, Kaizhou District, Yunyang Country, Fengjie Country, Wushan Country, Fengdu Country, Qianjiang District, Youyang Country, Pengshui Country, Xiushan Country.
	Quadrant 2	LH	1	2.6%	Shapingba District.
	Quadrant 4	HL	1	2.6%	Wanzhou District.
	---	NS	9	23.7%	The city proper of Chongqing and the city cluster of three gorges reservoir area in northeast Chongqing.
2022	Quadrant 1	HH	13	34.2%	The city proper of Chongqing: Tongliang District, Rongchang District, Yongchuan District, Jiangjin District, Qijiang District, Ba'nan District, Nan'an District, Jiulongpo District, Bishan District, Beibei District, Shapingba District, Yubei District, Nanchuan District.
	Quadrant 3	LL	8	21.1%	The city cluster of Wuling Mountain area in south eastern Chongqing and the city cluster of three gorges reservoir area in northeast Chongqing: Wuxi Country, Yunyang Country, Fengjie Country, Wushan Country, Qianjiang District, Youyang Country, Pengshui Country, Xiushan Country.
	Quadrant 2	LH	2	5.3%	Tongnan District, Shapingba District.
	Quadrant 4	HL	1	2.6%	Wanzhou District.
	---	NS	14		The city proper of Chongqing and the city cluster of three gorges reservoir area in northeast Chongqing.

4 Conclusions

4.1 Conclusions

Pollutant emission reduction can effectively promote the synergy between the two strategic goals of the "double carbon" strategy and the construction of a beautiful China. This study analyzed the spatiotemporal heterogeneity of $PM_{2.5}$ and O_3 in Chongqing, and also explored the spatial aggregation and outlier distribution characteristics of pollutants. The main conclusions are as follows:

(1) Areas with high concentrations of both pollutants are concentrated in the city proper of Chongqing, and there are spatial distribution differences between districts and counties. In addition, there is a complex linear interaction between $PM_{2.5}$ and O_3, with an overall negative correlation.
(2) $PM_{2.5}$ and O_3 had significant positive spatial autocorrelation and aggregation characteristics during the study period. The scatter points in the Moran's I scatter plot are mainly distributed in the first and third quadrants. This indicates that districts and counties with high (low) concentrations of $PM_{2.5}$ and O_3 are surrounded by districts and counties with high (low) concentrations.
(3) The spatial aggregation characteristics of O_3 were significantly stronger than those of $PM_{2.5}$ across the entire district. Meanwhile, the distribution of $PM_{2.5}$ showed a pattern of higher levels in the west and lower levels in the east. In addition, the areas where $PM_{2.5}$ and O_3 showed spatial aggregation areas showed high significance.

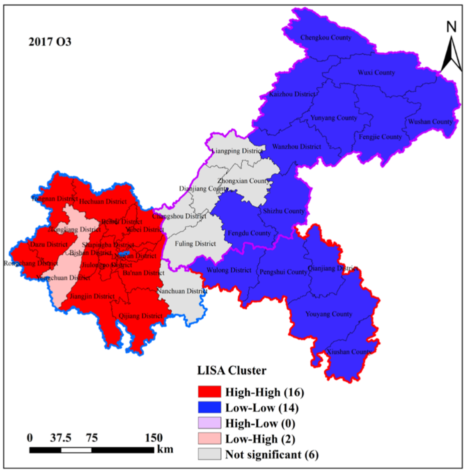

(a) 2017

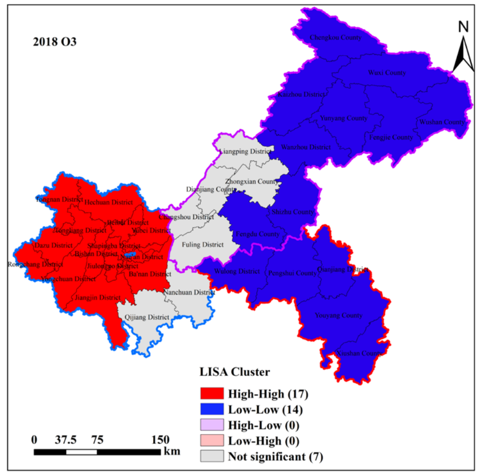

(b) 2018

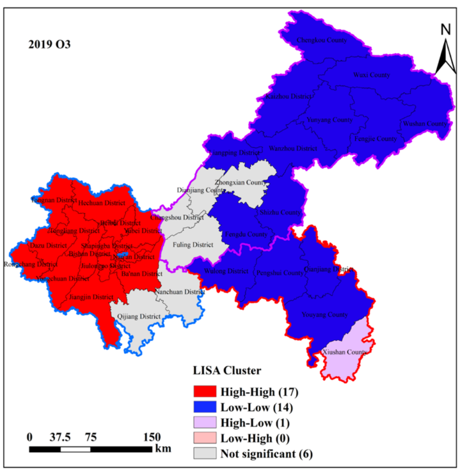

(c) 2019

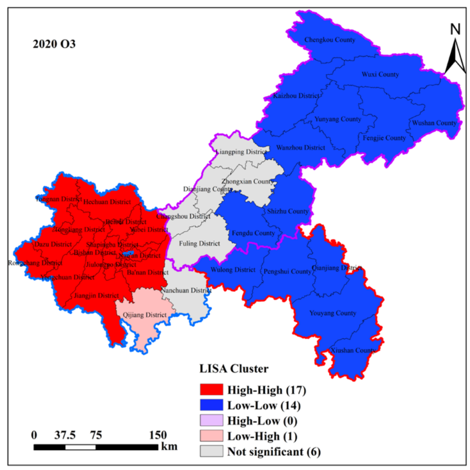

(d) 2020

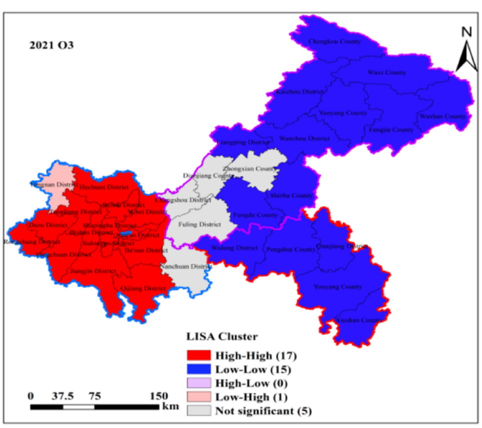

(e) 2021

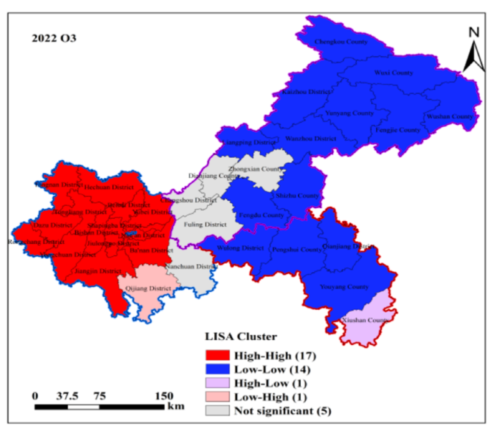

(f) 2022

Fig. 15 LISA cluster map of O_3 concentration (2017-2022). Note: The number represented the number of corresponding districts and counties

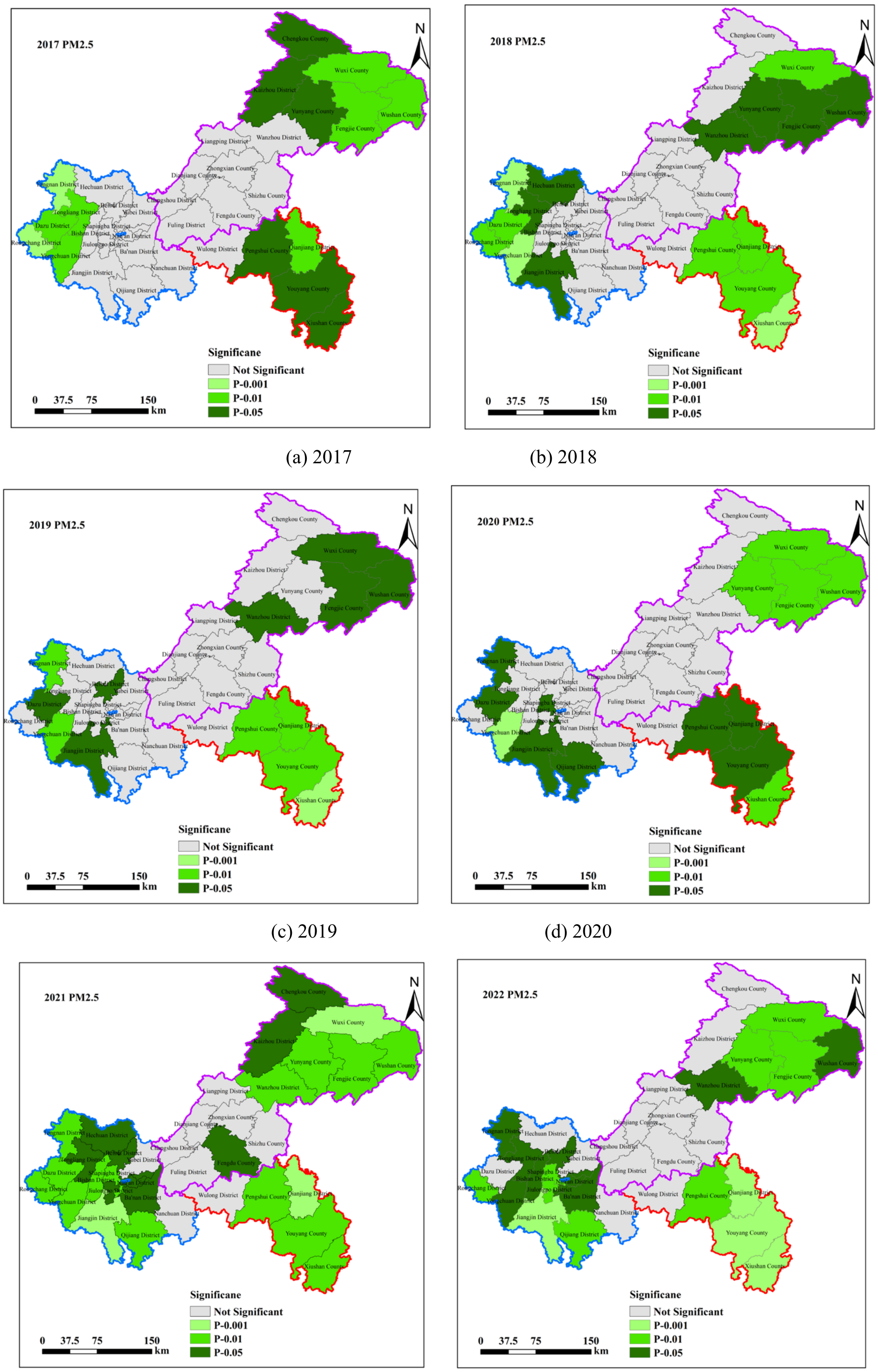

(a) 2017 (b) 2018

(c) 2019 (d) 2020

(e) 2020 (f) 2022

Fig. 16 Spatial significance characteristics map for $PM_{2.5}$ concentration (2017-2022)

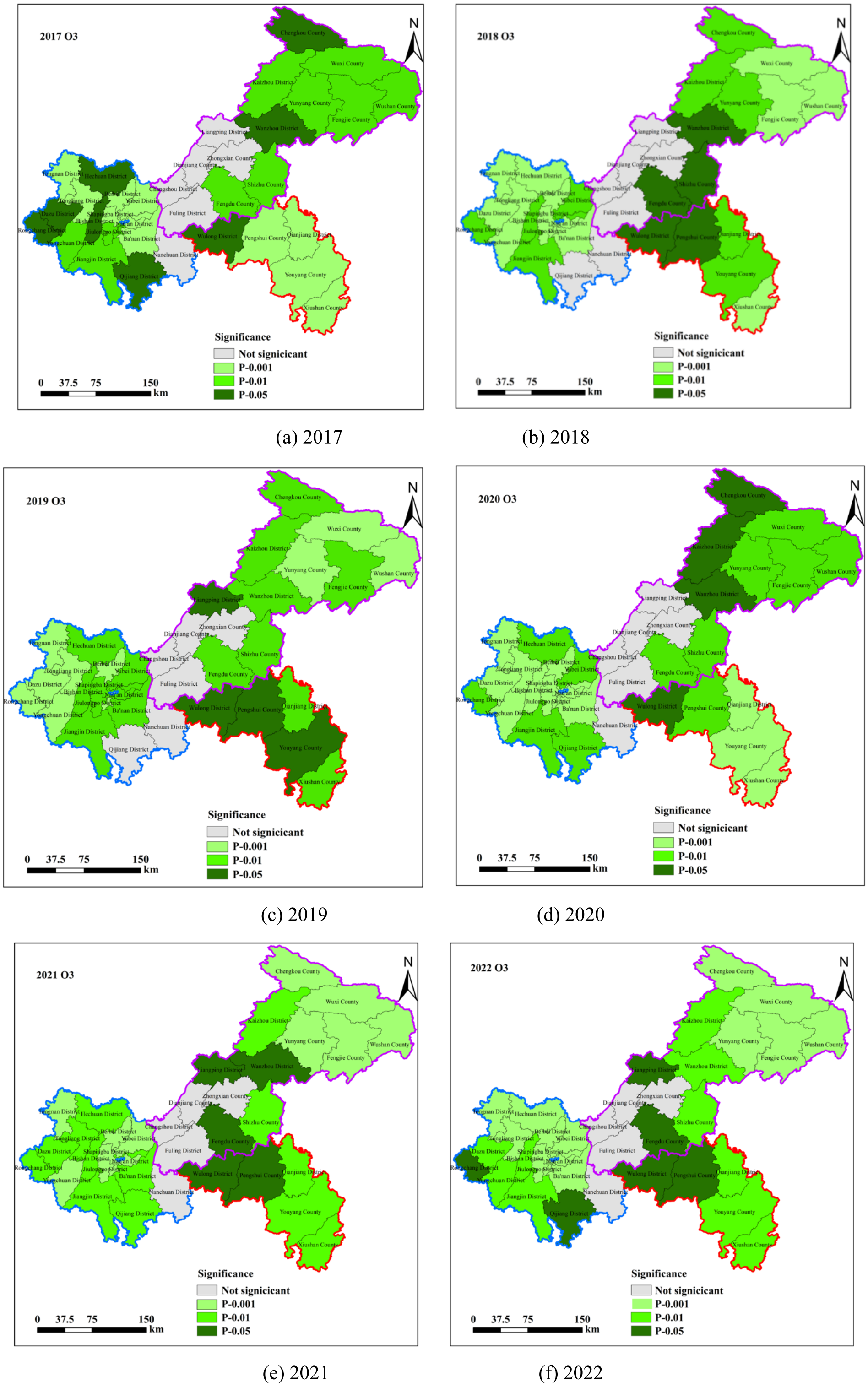

(a) 2017 (b) 2018

(c) 2019 (d) 2020

(e) 2021 (f) 2022

Fig. 17 Spatial significance characteristics map for O_3 concentration (2017-2022)

4.2 Suggestion and Prospects

Cross-border governance and regional linkage are better ways to control $PM_{2.5}$ and O_3 pollution. This study puts forward recommendations for joint prevention and control of air pollution from multiple perspectives at the provincial, regional, district and county levels. (1) Collaborative emission reduction of multiple pollutants is the fundamental way to curb $PM_{2.5}$ and O_3 composite pollution. Chongqing should use carbon neutrality strategies to continue to promote deep NOx emission reductions and reduce oxidation to achieve long-term root causes. (2) From the perspective of regional development, local governments particularly need to combine in-depth governance with differentiated management and control when formulating and implementing emission reduction policies. Targeting key seasons and key processes, differentiated control measures need to be taken from the aspects of region, time, source, variety, etc. (3) For individual districts and counties, local governments should implement scientific and refined control measures based on local conditions. Special attention should be paid to industries with high pollution emissions (transportation, steel industry, etc.) and enterprises with good emission reduction results. The selection of this study area is typical and detailed, and the spatiotemporal heterogeneity characteristics and spatial autocorrelation characteristics of $PM_{2.5}$ and O_3 concentrations can be obtained more clearly and intuitively. However, $PM_{2.5}$ and O_3 pollution are affected by the coupling of multiple complex factors. Therefore, in the next step, it is necessary to continue to explore the sensitivity relationship of the precursor control categories, namely O_3-NOX-VOCs, and the emission reduction ratio. In addition, carrying out collaborative carbon pollution reduction ($PM_{2.5}$-O_3-carbon collaborative reduction) in the Chengdu-Chongqing region is also an urgent issue that needs to be continuously discussed under the “dual carbon” goal.

Acknowledgement The authors would like to acknowledge to Xichang University, Sichuan Province, China and Department of Chemical and Environmental Engineering, Universiti Putra Malaysia for assistance and helpful with supporting to the writing of this article.

Funding Open access funding provided by The Ministry of Higher Education Malaysia and Universiti Putra Malaysia. This work was supported by the National Natural Science Foundation, China [grant numbers: 41967033]; the Municipal research project of Xichang Sichuan Province, China [grant numbers: 18JSYJ09]; the Project of Sichuan Meteorological Disaster Forecasting, Early Warning and Emergency Management Research Center, Sichuan Province, China [grant numbers: ZHYJ21-YB08; ZHYJ24-YB02]; Sichuan Provincial Philosophy and Social Sciences Planning Project “Construction of Beautiful Sichuan” [grant numbers: SC25ST016]; Sichuan Higher Education Social Science Key Research Base Chengdu-Chongqing Economic Circle Science and Technology Innovation and New Economy Research Center Project [grant numbers: CYCX2024ZC23]; Open Fund Project of Sichuan Mineral Resources Research Center, China [grant numbers: SCKCZY2025-ZC004]; Funded by Chengdu Research Center for Integrating into the New Pattern of Dual Circulation Development and Sichuan Research Center for Integrating into the New Pattern of Dual Circulation Development [grant numbers: SXH202514] and the scientific research project of Xichang University, China [grant numbers: YBZ202125].

Data Availability Data openly available in a public repository.

Declarations

Ethics Approval Not applicable. My manuscript does not report on or involve the use of any animal or human data or tissue.

Consent to Participate Not applicable.

Consent for Publication Not applicable.

Competing interests The authors declare that they have no known competing financial interests or personal relationships that could have appeared to influence the work reported in this paper.

References

Ai, M., Chen, X., & Yu, Q. (2024). Spatial correlation analysis between human disturbance intensity (HDI) and ecosystem services value (ESV) in the Chengdu-Chongqing urban agglomeration. *Ecological Indicators, 158*, Article 111555. https://doi.org/10.1016/j.ecolind.2024.111555

Bai, X., Chen, H., & Oliver, B. G. (2022a). The health effects of traffic-related air pollution: A review focused the health effects of going green. *Chemosphere, 289*, 133082. https://doi.org/10.1016/j.chemosphere.2021.133082

Bai, Y., Wang, Z., Xie, F., Cen, L., Xie, Z., Zhou, X., He, J., & Lü, C. (b). Changes in stoichiometric characteristics of ambient air pollutants pre-to post-COVID-19 in China. *Environmental Research, 209*(2), Article 112806. https://doi.org/10.1016/j.envres.2022.112806

Boniardi, L., Campo, L., Olgiati, L., Longhi, F., Scuffi, C., & Fustinoni, S. (2023). Biological monitoring and personal exposure to traffic-related air pollutants of elementary school-age children living in a metropolitan area. *Science of the Total Environment*. https://doi.org/10.1016/j.scitotenv.2022.159654

Chen, D., Zhou, L., Wang, C., Liu, H., Qiu, Y., Shi, G., Song, D., Tan, Q., & Yang, F. (2022). Characteristics of ambient volatile organic compounds during spring O_3 pollution episode in Chengdu, China. *Journal of Environmental Sciences (China), 114*(x), 115–125. https://doi.org/10.1016/j.jes.2021.08.014

China Clean Air Policy Partnership. (2021). A Synergistic Roadmap for Carbon Neutrality and Clean Air in China.

Chu, L., Chen, K., Yang, Z., Crowley, S., & Dubrow, R. (2024). A unified framework for assessing interaction effects among environmental exposures in epidemiologic studies: A case study on temperature, air pollution, and kidney-related conditions in New York state. *Environmental Research, 248*, Article 118324. https://doi.org/10.1016/j.envres.2024.118324

Deng, C., Qin, C., Li, Z., & Li, K. (2022a). Spatiotemporal variations of $PM_{2.5}$ pollution and its dynamic relationships with meteorological conditions in Beijing-Tianjin-Hebei region. *Chemosphere, 301*, 1–9. https://doi.org/10.1016/j.chemosphere.2022.134640

Deng, C., Tian, S., Li, Z., & Li, K. (b). Spatiotemporal characteristics of $PM_{2.5}$ and ozone concentrations in Chinese urban clusters. *Chemosphere*. https://doi.org/10.1016/j.chemosphere.2022.133813

Dettori, M., Deiana, G., Balletto, G., Borruso, G., Murgante, B., Arghittu, A., Azara, A., & Castiglia, P. (2021). Air pollutants and risk of death due to COVID-19 in Italy. *Environmental Research, 192*, 110459. https://doi.org/10.1016/j.envres.2020.110459

Ding, J., Huang, W., Zhao, J., Li, L., Xiong, G., Jiang, C., Ye, D., Li, D., Wang, J., Yu, J., & Liu, R. (2022). Characteristics and source origins of carbonaceous aerosol in fine particulate matter in a megacity, Sichuan Basin, southwestern China. *Atmospheric. Pollution Research*. https://doi.org/10.1016/j.apr.2021.101266

Dong, K., Hochman, G., Kong, X., Sun, R., & Wang, Z. (2019). Spatial econometric analysis of China's PM10 pollution and its influential factors: Evidence from the provincial level. *Ecological Indicators, 96*, 317–328. https://doi.org/10.1016/j.ecolind.2018.09.014

Dong, K., Sun, R., Dong, C., Li, H., Zeng, X., & Ni, G. (2018). Environmental Kuznets curve for $PM_{2.5}$ emissions in Beijing, China: What role can natural gas consumption play? *Ecological Indicators, 93*, 591–601. https://doi.org/10.1016/j.ecolind.2018.05.045

Energy Foundation China. (2020). Synthesis Report 2020 on China's Carbon Neutrality: China's New Growth Pathway: From the 14th Five Year Plan to Carbon Neutrality. https://www.efchina.org/Reports-en/report-lceg-20201210-en

Fan, J., Shang, Y., Zhang, X., Wu, X., Zhang, M., Cao, J., Luo, B., Zhang, X., Wang, S., Li, S., Liu, H., & Wu, P. (2020). Joint pollution and source apportionment of $PM_{2.5}$ among three different urban environments in Sichuan Basin, China. *Science of the Total Environment, 714*, 136305. https://doi.org/10.1016/j.scitotenv.2019.136305

Fan, J., Shen, M., Yan, T., Zhang, K., Zhang, T., Gong, C., Tian, X., Shang, Y., Yang, X., Shao, P., Tang, W., Li, M., & Wang, S. (2024). A mapping method for emission inventory and its application in air quality modeling. *Atmospheric Pollution Research, 15*(4), 102056. https://doi.org/10.1016/j.apr.2024.102056

Feng, R., & Fang, X. (2022). China's pathways to synchronize the emission reductions of air pollutants and greenhouse gases: Pros and cons. *Resources, Conservation and Recycling, 184*, 106392. https://doi.org/10.1016/j.resconrec.2022.106392

Feng, Y., Ning, M., Lei, Y., Sun, Y., Liu, W., & Wang, J. (2019). Defending blue sky in China: Effectiveness of the "Air Pollution Prevention and Control Action Plan" on air quality improvements from 2013 to 2017. *Journal of Environmental Management, 252*, 109603. https://doi.org/10.1016/j.jenvman.2019.109603

Feng, X., Zhang, X., & Wang, J. (2023a). Update of SO_2 emission inventory in the Megacity of Chongqing, China by inverse modeling. *Atmospheric Environment, 294*, 119519. https://doi.org/10.1016/j.atmosenv.2022.119519

Feng, Y., Ning, M., Xue, W., Cheng, M., & Lei, Y. (b). Developing China's roadmap for air quality improvement: A review on technology development and future prospects. *Journal of Environmental Sciences (China), 123*, 510–521. https://doi.org/10.1016/j.jes.2022.10.028

Fu, Z., & Li, R. (2020). The contributions of socioeconomic indicators to global $PM_{2.5}$ based on the hybrid method of spatial econometric model and geographical and temporal weighted regression. *Science of the Total Environment, 703*, Article 135481. https://doi.org/10.1016/j.scitotenv.2019.135481

Gao, S., Yu, J., Yang, W., Qu, F., Chen, L., Sun, Y., Zhang, H., Mao, J., Zhao, H., Azzi, M., & Bai, Z. (2022). Background concentration of atmospheric $PM_{2.5}$ in the Beijing–Tianjin–Hebei urban agglomeration: Levels, variation trends, and influences of meteorology and emission. *Atmospheric Pollution Research, 13*(11), Article 101583. https://doi.org/10.1016/j.apr.2022.101583

Gou, K., & Liu, Y. (2022). Study on the policy of air pollution control in Chengdu–Chongqing Economic Circle, China. *Energy Reports, 8*, 68–76. https://doi.org/10.1016/j.egyr.2022.10.116

Han, S., Park, Y., Noh, N., Kim, J. H., Kim, J. J., Kim, B. M., & Choi, W. (2023). Spatiotemporal variability of the $PM_{2.5}$ distribution and weather anomalies during severe pollution events: Observations from 462 air quality monitoring stations across South Korea. *Atmospheric Pollution Research, 14*(3), Article 101676. https://doi.org/10.1016/j.apr.2023.101676

Hu, J., Zhao, T., Liu, J., Cao, L., Wang, C., Li, Y., Shi, C., Tan, C., Sun, X., Shu, Z., & Li, J. (2022). Exploring the ozone pollution over the western Sichuan Basin, Southwest China: The impact of diurnal change in mountain-plains solenoid. *Science of the Total Environment, 839*, Article 156264. https://doi.org/10.1016/j.scitotenv.2022.156264

Huang, J., Li, X., Zhang, Y., Zhai, S., Wang, W., Zhang, T., Yin, F., & Ma, Y. (2023). Socio-demographic characteristics and inequality in exposure to $PM_{2.5}$: A case study in the Sichuan basin, China. *Environmental Pollution, 316*(P2), Article 120630. https://doi.org/10.1016/j.envpol.2022.120630

Ji, G., Tian, L., Zhao, J., Yue, Y., & Wang, Z. (2019). Detecting spatiotemporal dynamics of $PM_{2.5}$ emission data in China using DMSP-OLS nighttime stable light data. *Journal of Cleaner Production, 209*, 363–370. https://doi.org/10.1016/j.jclepro.2018.10.285

Huynh, C. M., Le, Q. N., Huong, T., & Lam, T. (2023). Is air pollution a government failure or a market failure ? Global evidence from a multi-dimensional analysis. *Energy Policy, 173*, 113384. https://doi.org/10.1016/j.enpol.2022.113384

Ji, S., Zhang, Z., Meng, F., Luo, H., Yang, M., Wang, D., Tan, Q., Deng, Y., & Gong, Z. (2024). Scenario simulation and synergistic effect analysis of CO_2 and atmospheric pollutant emission reduction in urban transport sector: A case study of Chengdu, China. *Journal of Cleaner Production, 438*, Article 140841. https://doi.org/10.1016/j.jclepro.2024.140841

Jin, H., Zhong, R., Liu, M., Ye, C., & Chen, X. (2022). Spatiotemporal distribution characteristics of $PM_{2.5}$ concentration in China from 2000 to 2018 and its impact on population. *Journal of Environmental Management, 323*, Article 116273. https://doi.org/10.1016/j.jenvman.2022.116273

Kazemi Shariat Panahi, H., Dehhaghi, M., Lam, S. S., Peng, W., Aghbashlo, M., Tabatabaei, M., & Guillemin, G. J. (2022). Oncolytic viruses as a promising therapeutic strategy against the detrimental health impacts of air pollution: The case of glioblastoma multiforme. *Seminars in Cancer Biology, 86*(P3), 1122–1142. https://doi.org/10.1016/j.semcancer.2021.05.013

Kumar, A., Dhakhwa, S., & Dikshit, A. K. (2022). Comparative evaluation of fitness of interpolation techniques of ArcGIS using leave-one-out scheme for air quality mapping. *Journal of Geovisualization and Spatial Analysis, 6*(1), 1–11. https://doi.org/10.1007/s41651-022-00102-4

Lee, H. J., Kuwayama, T., & FitzGibbon, M. (2023). Trends of ambient O_3 levels associated with O_3 precursor gases and meteorology in California: Synergies from ground and satellite observations. *Remote Sensing of Environment, 284*, Article 113358. https://doi.org/10.1016/j.rse.2022.113358

LI, Y., An, X., Zhang, P., Yang, J., Wang, C., & Li, J. (2021a). Influence of East Asian winter monsoon on particulate matter pollution in typical regions of China. *Atmospheric Environment, 260*, Article 118213. https://doi.org/10.1016/j.atmosenv.2021.118213

Li, W., Dong, F., & Ji, Z. (2021b). Research on coordination level and influencing factors spatial heterogeneity of China's urban CO_2 emissions. *Sustainable Cities and Society, 75*, Article 103323. https://doi.org/10.1016/j.scs.2021.103323

Li, W., Sun, W., Li, G., Cui, P., Wu, W., & Jin, B. (2017). Temporal and spatial heterogeneity of carbon intensity in China's construction industry. *Resources, Conservation and Recycling, 126*, 162–173. https://doi.org/10.1016/j.resconrec.2017.07.043

Li, T., Zhang, Q., Peng, Y., Guan, X., Li, L., & Mu, J. (2023). Contributions of Various Driving Factors to Air Pollution Events : Interpretability Analysis from Big Data Research Center for Ecology and Environment. *Environment International*, 107861. https://doi.org/10.1016/j.envint.2023.107861

Liao, T., Gui, K., Jiang, W., Wang, S., Wang, B., Zeng, Z., Che, H., Wang, Y., & Sun, Y. (2018). Air stagnation and its impact on air quality during winter in Sichuan and Chongqing, southwestern China. *Science of the Total Environment, 635*, 576–585. https://doi.org/10.1016/j.scitotenv.2018.04.122

Lin, H., Zhu, J., Jiang, P., Cai, Z., Yang, X., Yang, X., Zhou, Z., & Wei, J. (2022). Assessing drivers of coordinated control of ozone and fine particulate pollution: Evidence from Yangtze River Delta in China. *Environmental Impact Assessment Review, 96*, Article 106840. https://doi.org/10.1016/j.eiar.2022.106840

Liu, S., He, N., Shi, Y., & Li, G. (2021). The roles logistics agglomeration and technological progress play in air pollution — New evidence in sub-regions of Chongqing. China. *Journal of Cleaner Production, 317*, Article 128414. https://doi.org/10.1016/j.jclepro.2021.128414

Liu, Z., Liang, Q., Liao, H., Yang, W., & Lu, C. (2023). Effects of short-term and long-term exposure to ambient air pollution and temperature on long recovery duration in COVID-19 patients. *Environmental Research, 216*(P4), Article 114781. https://doi.org/10.1016/j.envres.2022.114781

Liu, Y., Qiu, P., Li, C., Li, X., Ma, W., Yin, S., Yu, Q., Li, J., & Liu, X. (2022). Evolution and variations of atmospheric VOCs and O_3 photochemistry during a summer O_3 event in a county-level city, Southern China. *Atmospheric Environment, 272*, Article 118942. https://doi.org/10.1016/j.atmosenv.2022.118942

Luo, K., Wang, Z., & Wu, J. (2022). Association of population migration with air quality: Role of city attributes in China during COVID-19 pandemic (2019–2021). *Atmospheric Pollution Research, 13*(5), Article 101419. https://doi.org/10.1016/j.apr.2022.101419

Ma, M., Liu, M., Song, X., Liu, M., Fan, W., Wang, Y., Xing, H., Meng, F., & Lv, Y. (2024). Spatiotemporal patterns and quantitative analysis of influencing factors of $PM_{2.5}$ and O_3 pollution in the North China Plain. *Atmospheric Pollution Research, 15*(1), Article 101950. https://doi.org/10.1016/j.apr.2023.101950

Ma, X., Longley, I., Gao, J., Kachhara, A., & Salmond, J. (2019). A site-optimised multi-scale GIS based land use regression model for simulating local scale patterns in air pollution. *Science of the Total Environment, 685*, 134–149. https://doi.org/10.1016/j.scitotenv.2019.05.408

Ma, D., Wang, T., Xu, B., Song, R., Gao, L., Chen, H., Ren, X., Li, S., Zhuang, B., Li, M., Xie, M., & Saikawa, E. (2023). The mutual interactions among ozone, fine particulate matter, and carbon dioxide on summer monsoon climate in East Asia. *Atmospheric Environment, 299*, Article 119668. https://doi.org/10.1016/j.atmosenv.2023.119668

Maji, K. J., Arora, M., & Dikshit, A. K. (2018). Premature mortality attributable to $PM_{2.5}$ exposure and future policy roadmap for 'airpocalypse' affected Asian megacities. *Process Safety and Environmental Protection, 118*, 371–383. https://doi.org/10.1016/j.psep.2018.07.009

Martori, J. C., Lagonigro, R., & Iglesias-Pascual, R. (2022). Social status and air quality in Barcelona: A socio-ecological approach. *Sustainable Cities and Society, 87*, Article 104210. https://doi.org/10.1016/j.scs.2022.104210

Mi, Y., Sun, K., Li, L., Lei, Y., Wu, S., Tang, W., Wang, Y., & Yang, J. (2021). Spatiotemporal pattern analysis of $PM_{2.5}$ and the driving factors in the middle Yellow River urban agglomerations. *Journal of Cleaner Production*. https://doi.org/10.1016/j.jclepro.2021.126904

Mi, T., Tang, D., Fu, J., Zeng, W., Grieneisen, M. L., Zhou, Z., Jia, F., Yang, F., & Zhan, Y. (2024). Data augmentation for bias correction in mapping $PM_{2.5}$ based on satellite retrievals and ground observations. *Geoscience Frontiers, 15*(1), Article 101686. https://doi.org/10.1016/j.gsf.2023.101686

Mi, K., Zhuang, R., Zhang, Z., Gao, J., & Pei, Q. (2019). Spatiotemporal characteristics of $PM_{2.5}$ and its associated gas pollutants, a case in China. *Sustainable Cities and Society, 45*(100), 287–295. https://doi.org/10.1016/j.scs.2018.11.004

Montone, R. A., Rinaldi, R., Bonanni, A., Severino, A., Pedicino, D., Crea, F., & Liuzzo, G. (2023). Impact of air pollution on ischemic heart disease: Evidence, mechanisms, clinical perspectives. *Atherosclerosis, 366*, 22–31. https://doi.org/10.1016/j.atherosclerosis.2023.01.013

Ning, G., Wang, S., Ma, M., Ni, C., Shang, Z., Wang, J., & Li, J. (2018). Characteristics of air pollution in different zones of Sichuan Basin, China. *Science of the Total Environment, 612*, 975–984. https://doi.org/10.1016/j.scitotenv.2017.08.205

Peng, C., Yang, F., Tian, M., Shi, G., Li, L., Huang, R. J., Yao, X., Luo, B., Zhai, C., & Chen, Y. (2020). Brown carbon aerosol in two megacities in the Sichuan Basin of southwestern China: Light absorption properties and implications. *Science of the Total Environment, 719*, Article 137483. https://doi.org/10.1016/j.scitotenv.2020.137483

Qiao, B., Chen, Y., Tian, M., Wang, H., Yang, F., Shi, G., Zhang, L., Peng, C., Luo, Q., & Ding, S. (2019). Characterization of water soluble inorganic ions and their evolution processes during $PM_{2.5}$ pollution episodes in a small city in southwest China. *Science of the Total Environment, 650*, 2605–2613. https://doi.org/10.1016/j.scitotenv.2018.09.376

Qiao, X., Liu, L., Yang, C., Yuan, Y., Zhang, M., Guo, H., Tang, Y., Ying, Q., Zhu, S., & Zhang, H. (2021). Responses of fine particulate matter and ozone to local emission reductions in the Sichuan Basin, southwestern China. *Environmental Pollution, 277*, Article 116793. https://doi.org/10.1016/j.envpol.2021.116793

Qi, G., Che, J., & Wang, Z. (2023). Differential effects of urbanization on air pollution: Evidences from six air pollutants in mainland China. *Ecological Indicators, 146*(2), 109924. https://doi.org/10.1016/j.ecolind.2023.109924

Rahman, M., Islam, M., Shimanto, M. H., Ferdous, J., Rahman, A. A. N. S., Sagor, P. S., & Chowdhury, T. (2021). A global analysis on the effect of temperature, socio-economic and environmental factors on the spread and mortality rate of the COVID-19 pandemic. *Environment, Development and Sustainability, 23*(6), 9352–9366. https://doi.org/10.1007/s10668-020-01028-x

Ran, J., Zhao, S., Han, L., Chen, D., Yang, Z., Yang, L., Wang, M. H., & He, D. (2020). The ambient ozone and COVID-19 transmissibility in China: A data-driven ecological study of 154 cities. *Journal of Infection, 81*(3), e9–e11. https://doi.org/10.1016/j.jinf.2020.07.011

Ren, L., & Matsumoto, K. (2020). Effects of socioeconomic and natural factors on air pollution in China: A spatial panel data analysis. *Science of the Total Environment, 740*, Article 140155. https://doi.org/10.1016/j.scitotenv.2020.140155

Shi, Y., Bilal, M., Ho, H. C., & Omar, A. (2020). Urbanization and regional air pollution across South Asian developing countries – A nationwide land use regression for ambient $PM_{2.5}$ assessment in Pakistan. *Environmental Pollution, 266*, Article 115145. https://doi.org/10.1016/j.envpol.2020.115145

Shi, X., Zheng, Y., Lei, Y., Xue, W., Yan, G., Liu, X., Cai, B., Tong, D., & Wang, J. (2021). Air quality benefits of achieving carbon neutrality in China. *Science of the Total Environment, 795*, Article 148784. https://doi.org/10.1016/j.scitotenv.2021.148784

Si, J., Zhang, L., Zhang, S., Li, Y., Zhang, Z., He, Z., Chen, Y., & Zhan, H. (2024). Response of air pollution to meteorological conditions and socioeconomic activities associated to the COVID-19 outbreak in the Yangtze River Economic Belt. *Atmospheric Environment, 323*, Article 120390. https://doi.org/10.1016/j.atmosenv.2024.120390

Song, J., Qi, Z., Gai, Y., & Chen, S. (2022). Shared network and supply chain features for synergetic control of carbon and air pollutant emissions. *Science of the Total Environment, 827*, Article 154391. https://doi.org/10.1016/j.scitotenv.2022.154391

Su, R., Lu, K. D., Yu, J. Y., Tan, Z. F., Jiang, M. Q., Li, J., Xie, S. D., Wu, Y. S., Zeng, L. M., Zhai, C. Z., & Zhang, Y. H. (2018). Exploration of the formation mechanism and source attribution of ambient ozone in Chongqing with an observation-based model. *Science China Earth Sciences, 61*, 23–32. https://doi.org/10.1007/s11430-017-9104-9

Tamir, T. T., & Atallel, K. A. (2023). Spatial variations and determinants of optimal antenatal care service utilisation in Ethiopia: Spatial and survey regression analysis. *Public Health, 220*, 18–26. https://doi.org/10.1016/j.puhe.2023.04.010

Tan, Z., Lu, K., Jiang, M., Su, R., Dong, H., Zeng, L., Xie, S., Tan, Q., & Zhang, Y. (2018). Exploring ozone pollution in Chengdu, southwestern China: A case study from radical chemistry to O_3-VOC-NOx sensitivity. *Science of the Total Environment, 636*, 775–786. https://doi.org/10.1016/j.scitotenv.2018.04.286

Tan, S., Xie, D., Ni, C., Zhao, G., Shao, J., Chen, F., & Ni, J. (2023). Spatiotemporal characteristics of air pollution in Chengdu-Chongqing urban agglomeration (CCUA) in Southwest, China: 2015–2021. *Journal of Environmental Management, 325*(PA), Article 116503. https://doi.org/10.1016/j.jenvman.2022.116503

Tang, L., Ruan, J., Bo, X., Mi, Z., Wang, S., Dong, G., & Davis, S. J. (2022). Plant-level real-time monitoring data reveal substantial abatement potential of air pollution and CO_2 in China's cement sector. *One Earth, 5*(8), 892–906. https://doi.org/10.1016/j.oneear.2022.07.003

Tian, Y., Yao, X., & Chen, L. (2019). Analysis of spatial and seasonal distributions of air pollutants by incorporating urban morphological characteristics. *Computers, Environment and Urban Systems, 75*, 35–48. https://doi.org/10.1016/j.compenvurbsys.2019.01.003

Wang, Q., Dong, W., Yang, K., Ren, Z., Huang, D., Zhang, P., & Wang, J. (2021). Temporal and spatial analysis of COVID-19 transmission in China and its influencing factors. *International Journal of Infectious Diseases, 105*, 675–685. https://doi.org/10.1016/j.ijid.2021.03.014

Wang, H., Gu, K., Sun, H., & Xiao, H. (2023). Reconfirmation of the symbiosis on carbon emissions and air pollution: A spatial spillover perspective. *Science of the Total Environment, 858*, Article 159906. https://doi.org/10.1016/j.scitotenv.2022.159906

Wang, Z. B., Li, J. X., & Liang, L. W. (2020). Spatio-temporal evolution of ozone pollution and its influencing factors in the Beijing-Tianjin-Hebei Urban Agglomeration. *Environmental Pollution, 256*, Article 113419. https://doi.org/10.1016/j.envpol.2019.113419

Wang, Y., Wang, J., Zhang, M., & Shi, L. (2019). Spatial correlation analysis of energy consumption and air pollution in Beijing-Tianjin-Hebei region. *Energy Procedia, 158*, 4280–4285. https://doi.org/10.1016/j.egypro.2019.01.797

Wong, P., Su, H., Lung, S. C., & Wu, C. (2023). Science of the total environment an ensemble mixed spatial model in estimating long-term and diurnal variations of $PM_{2.5}$ in Taiwan. *Science of the Total Environment, 866*(1), Article 161336. https://doi.org/10.1016/j.scitotenv.2022.161336

Wu, B., Liu, C., Zhang, J., Du, J., & Shi, K. (2021). The multifractal evaluation of $PM_{2.5}$-O_3 coordinated control capability in China. *Ecological Indicators*. https://doi.org/10.1016/j.ecolind.2021.107877

Xiao, C., Zhou, J., Meng, F., Cullen, J., Wang, X., & Zhu, Y. (2023). Regional characteristics and spatial correlation of haze pollution: Interpretative system analysis in cities of Fenwei Plain in China. *Science of the Total Environment, 869*, Article 161779. https://doi.org/10.1016/j.scitotenv.2023.161779

Xu, X., Lin, Y., Meng, B., Feng, X., Xu, Z., Jiang, Y., Zhong, W., Hu, Y., & Qiu, G. (2018). The impact of an abandoned mercury mine on the environment in the Xiushan region, Chongqing, southwestern China. *Applied Geochemistry, 88*, 267–275. https://doi.org/10.1016/j.apgeochem.2017.04.005

Xu, J., Lv, T., Hou, X., Deng, X., Li, N., & Liu, F. (2022). Spatiotemporal characteristics and influencing factors of renewable energy production in China: A spatial econometric analysis. *Energy Economics*. https://doi.org/10.1016/j.eneco.2022.106399

Xu, C., Yang, J., He, L., Wei, W., Yang, Y., Yin, X., Yang, W., & Lin, A. (2021). Carbon capture and storage as a strategic reserve against China's CO_2 emissions. *Environmental Development, 37*, 1–9. https://doi.org/10.1016/j.envdev.2020.100608

Xu, H., Zeng, W., Guo, B., Hopke, P. K., Qiao, X., Choi, H., Luo, B., Zhang, W., & Zhao, X. (2020). Improved risk communications with a Bayesian multipollutant Air Quality Health Index. *Science of the Total Environment, 722*, Article 137892. https://doi.org/10.1016/j.scitotenv.2020.137892

Yang, X., Wang, S., Zhang, W., & Yu, J. (2017). Are the temporal variation and spatial variation of ambient SO_2 concentrations determined by different factors? *Journal of Cleaner Production, 167*, 824–836. https://doi.org/10.1016/j.jclepro.2017.08.215

Yang, J., Yang, Z., Qi, L., Li, M., Liu, D., Liu, X., Tong, S., Sun, Q., Feng, L., Ou, C. Q., & Liu, Q. (2023). Influence of air pollution on influenza-like illness in China: A nationwide time-series analysis. *EBioMedicine, 87*, 1–11. https://doi.org/10.1016/j.ebiom.2022.104421

Yang, X., Yang, Y., Xu, S., Karimian, H., Zhao, Y., Jin, L., Xu, Y., & Qi, Y. (2024). Unveiling the air pollution tapestry in China: A comprehensive assessment of spatiotemporal variations through geographically and temporally weighted regression. *Atmospheric Pollution Research, 15*(2), Article 101987. https://doi.org/10.1016/j.apr.2023.101987

Yi, H., Zhao, L., Qian, Y., Zhou, L., & Yang, P. (2022). How to achieve synergy between carbon dioxide mitigation and air pollution control? Evidence from China. *Sustainable Cities and Society, 78*, Article 103609. https://doi.org/10.1016/j.scs.2021.103609

Yu, S., Horing, J., Liu, Q., Dahowski, R., Davidson, C., Edmonds, J., Liu, B., Mcjeon, H., McLeod, J., Patel, P., & Clarke, L. (2019). CCUS in China's mitigation strategy: Insights from integrated assessment modeling. *International Journal of Greenhouse Gas Control, 84*, 204–218. https://doi.org/10.1016/j.ijggc.2019.03.004

Zeng, J., & Bao, R. (2021). The impacts of human migration and city lockdowns on specific air pollutants during the COVID-19 outbreak: A spatial perspective. *Journal of Environmental Management, 282*(2), Article 111907. https://doi.org/10.1016/j.jenvman.2020.111907

Zhan, C. C., Xie, M., Fang, D. X., Wang, T. J., Wu, Z., Lu, H., Li, M. M., Chen, P. L., Zhuang, B. L., Li, S., & Zhang, Z. Q. (2019). Synoptic weather patterns and their impacts on regional particle pollution in the city cluster of the Sichuan Basin, China. *Atmospheric Environment, 208*, 34–47. https://doi.org/10.1016/j.atmosenv.2019.03.033

Zhang, Y., Cai, J., Wang, S., He, K., & Zheng, M. (2017). Review of receptor-based source apportionment research of fine particulate matter and its challenges in China. *Science of the Total Environment, 586*, 917–929. https://doi.org/10.1016/j.scitotenv.2017.02.071

Zhang, L., Guo, X., Zhao, T., Gong, S., Xu, X., Li, Y., Luo, L., Gui, K., Wang, H., Zheng, Y., & Yin, X. (2019). A modelling study of the terrain effects on haze pollution in the Sichuan Basin. *Atmospheric Environment, 196*, 77–85. https://doi.org/10.1016/j.atmosenv.2018.10.007

Zhang, J., Li, H., Chen, L., Huang, X., Zhang, W., & Zhao, R. (2022). Particle composition, sources and evolution during the COVID-19 lockdown period in Chengdu, southwest China: Insights from single particle aerosol mass spectrometer data. *Atmospheric Environment, 268*, Article 118844. https://doi.org/10.1016/j.atmosenv.2021.118844

Zhang, N. N., Ma, F., Qin, C. B., & Li, Y. F. (2018). Spatiotemporal trends in $PM_{2.5}$ levels from 2013 to 2017 and regional demarcations for joint prevention and control of atmospheric pollution in China. *Chemosphere, 210*, 1176–1184. https://doi.org/10.1016/j.chemosphere.2018.07.142

Zhao, S., Pudasainee, D., Duan, Y., Gupta, R., Liu, M., & Lu, J. (2019). A review on mercury in coal combustion process: Content and occurrence forms in coal, transformation, sampling methods, emission and control technologies. *Progress in Energy and Combustion Science, 73*, 26–64. https://doi.org/10.1016/j.pecs.2019.02.001

Zhao, H., Wang, L., Zhang, Z., Qi, Q., & Zhang, H. (2022). Quantifying ecological and health risks of ground-level O_3 across China during the implementation of the "Three-year Action Plan for Cleaner Air." *Science of the Total Environment*. https://doi.org/10.1016/j.scitotenv.2022.153011

Zhou, Z., Tan, Q., Deng, Y., Wu, K., Yang, X., & Zhou, X. (2019). Emission inventory of anthropogenic air pollutant sources and characteristics of VOCs species in Sichuan Province, China. *Journal of Atmospheric Chemistry, 76*, 21–58. https://doi.org/10.1007/s10874-019-9386-7